

Lisa Dittmer, BSc

**Structure-function analysis and characterization of
two flavin-dependent enzymes:
HMF oxidase and L-amino acid deaminase**

MASTER'S THESIS

to achieve the university degree of

Diplom-Ingenieurin

Master's degree programme: Biotechnology

submitted to

Graz University of Technology

Supervisor

Priv.-Doz. Dipl.-Ing. Dr.nat.techn. Mario Klimacek

Institute of Biotechnology and Biochemical Engineering

AFFIDAVIT

I declare that I have authored this thesis independently, that I have not used other than the declared sources/resources, and that I have explicitly indicated all material which has been quoted either literally or by content from the sources used. The text document uploaded to TUGRAZonline is identical to the present master's thesis.

30th of July 2018

Date

A handwritten signature in blue ink that reads "Lisa Ollmer". The signature is written in a cursive style with a large initial 'L' and 'O'.

Signature

Acknowledgement

Foremost, I want to thank my thesis advisor Priv.-Doz. Dipl.-Ing. Dr.nat.techn. Mario Klimacek for supporting the opportunity to do the research for this thesis abroad. In addition, I would like to thank him for his patient guidance and advice during the whole writing process.

I would like to express my sincere gratitude to Prof. Dr. Ir. Marco Fraaije for providing the special opportunity and projects for a foreign master student to enable this work at the Biomolecular Sciences and Biotechnology Institute at the University of Groningen, Netherlands.

Special thanks goes to Willem Dijkman, PhD for the support and supervision of the research part of this thesis in the laboratory. Furthermore, I would like to thank all members of the Biotransformation and Biocatalysis working group for the great working atmosphere and their assistance.

I would also like to gratefully acknowledge Alwin for his continued support and constant encouragement during the process of conducting this thesis.

Last but not least, I would like to express my profound and everlasting gratitude to my parents Heidi and Edi and my sister Eva. They have always loved me unconditionally and gave me their unfailing support and understanding throughout my whole university education.

Abstract

Flavin-dependent enzymes, also known as flavoenzymes, are one of the most versatile group of enzymes used today in biocatalysis. They obtain their enzymatic ability by a (bound) cofactor in an often-unique active site to form a beneficial environment for chemical conversions. Their excellent properties with respect to efficiency and selectivity open up a wide range of opportunities in industrial applications. Through rationally improving their versatility, flavoenzymes are often replacing otherwise polluting chemical processes.

The demand for oil-based compounds is rising despite the rapid depletion of petrochemical reserves in the world. A most promising building block for the bio-based economy is 2,5-furandicarboxylic acid (FDCA), the precursor for the production of polymers such as bioplastic polyethylene furanoate (PEF). As of today, FDCA is produced from 5-hydroxymethylfurfural (HMF). A recently new described enzyme, 5-hydroxymethylfurfural oxidase (HMFO) is capable of oxidizing HMF to FDCA in three consecutive steps. To improve the conversion of HMF to FDCA seven variants of HMFO were created and analyzed. Resulting variants achieved FDCA yields up to 96%. Moreover, for two variants a higher thermal stability was observed.

Another challenge in biocatalysis is the production of enantiomerically pure amino acids for chiral pharmaceuticals and therapeutic drugs. L-amino acid deaminase (LAAD) from *Proteus myxofaciens* catalyzes the deamination of L-amino acids into the corresponding α -keto acid. This transmembrane enzyme shows no reported hydrogen peroxide production, which is usually formed in other oxidases. This raises the question of the classification of LAAD as a typical amine oxidase. Due to its insolubility in aqueous environments, enzyme properties were so far analyzed in whole cells. To facilitate enzyme-specific analysis soluble forms are required. To this end, three truncated enzyme variants were created and their expression behavior studied under different conditions and in different cell fractions. LAAD variants were not soluble and were predominantly found in the membrane fraction and as inclusion bodies. Results imply that these variants contained still functional transmembrane regions.

Zusammenfassung

Flavin-abhängige Enzyme, auch Flavoenzyme genannt, sind eine der vielseitigsten Enzymgruppen, die heute in der Biokatalyse eingesetzt werden. Sie erhalten ihre enzymatische Fähigkeit durch einen (gebundenen) Kofaktor in einem oft einzigartigen aktiven Zentrum, um eine günstige Umgebung für chemische Umwandlungen zu bilden. Ihre ausgezeichneten Eigenschaften in Bezug auf Effizienz und Selektivität eröffnen eine Vielzahl von Möglichkeiten in industriellen Anwendungen. Durch die rationelle Verbesserung ihrer Vielfältigkeit ersetzen Flavoenzyme oft andere sonst umweltschädliche chemische Prozesse.

Die Nachfrage nach ölbasierten Verbindungen steigt trotz der rapiden weltweiten Erschöpfung der petrochemischen Reserven. Ein vielversprechender Baustein für die biobasierte Wirtschaft ist 2,5-Furandicarbonsäure (FDCA), die Vorstufe für die Herstellung von Polymeren wie dem Biokunststoff Polyethylenfuranoat (PEF). Heute wird FDCA aus 5-Hydroxymethylfurfural (HMF) hergestellt. Ein kürzlich neu beschriebenes Enzym, 5-Hydroxymethylfurfuraloxidase (HMFO) ist in der Lage HMF in drei aufeinanderfolgenden Schritten zu FDCA zu oxidieren. Um die Umwandlung von HMF zu FDCA zu verbessern, wurden sieben HMFO Varianten erstellt und analysiert. Resultierende Varianten erreichen eine FDCA Ausbeute von bis zu 96%. Darüber hinaus wurde für zwei Varianten eine höhere thermische Stabilität beobachtet.

Eine weitere Herausforderung in der Biokatalyse ist die Herstellung von enantiomerenreinen Aminosäuren für chirale Pharmazeutika und Therapeutika.

L-Aminosäure-Deaminase (LAAD) aus *Proteus myxofaciens* katalysiert die Desaminierung von L-Aminosäuren in die entsprechende α -Ketosäure. Dieses Transmembranenzym zeigt keine berichtete Produktion von Wasserstoffperoxid, das üblicherweise bei anderen Oxidasen gebildet wird. Dies wirft die Frage nach der Klassifizierung von LAAD als eine typische Aminoxidase auf. Aufgrund der Unlöslichkeit in wässriger Umgebung von LAAD wurden die Enzymeigenschaften bisher in ganzen Zellen analysiert. Um die enzyspezifische Analyse zu erleichtern, sind lösliche Formen erforderlich. Zu diesem Zweck wurden drei verkürzte Enzymvarianten erstellt und ihr Expressionsverhalten unter verschiedenen

Bedingungen und in verschiedenen Zellfraktionen untersucht. LAAD Varianten waren nicht löslich und wurden vorwiegend in der Membranfraktion und als Einschlusskörperchen gefunden. Die Ergebnisse implizieren, dass diese Varianten noch funktionelle Transmembranregionen enthielten.

Table of contents

1	INTRODUCTION.....	1
1.1	Flavin-dependent enzymes	1
1.2	Flavin-based cofactors FAD and FMN.....	1
1.3	HMF oxidase and L-amino acid deaminase.....	3
2	MATERIALS	4
2.1	List of chemicals	4
2.2	Buffers, gels and gel markers	6
2.3	Microorganisms.....	7
2.4	Plasmids.....	8
2.5	Enzymes	9
2.6	Kits.....	10
2.7	Instruments.....	10
3	STRUCTURE-FUNCTION ANALYSIS OF HMF OXIDASE	14
3.1	Introduction.....	14
3.1.1	FDCA and HMF as building blocks for new polymers	14
3.1.2	The oxidation pathway of HMF to FDCA by HMF oxidase.....	15
3.1.3	HMF oxidase.....	15
3.1.4	Limitations in current HMF oxidase catalyzed FDCA production	16
3.2	Aim of work.....	18
3.3	Methods.....	19
3.3.1	Molecular biology procedures.....	19
3.3.1.1	Media preparation	19
3.3.1.1.1	Lysogeny broth medium	19
3.3.1.1.2	Terrific broth medium.....	19
3.3.1.2	Determination of cell density.....	19
3.3.1.3	Production of E. coli competent cells	20

3.3.1.4	Heat shock transformation	20
3.3.1.5	PCR product purification	21
3.3.1.6	Plasmid isolation and purification.....	21
3.3.1.7	Site directed mutagenesis.....	21
3.3.1.8	Expression	24
3.3.1.9	Purification	24
3.3.1.10	Gel electrophoresis	25
3.3.1.11	Agarose gel electrophoresis	25
3.3.1.12	SDS-PAGE gel electrophoresis	26
3.3.1.13	Sonication	26
3.3.2	Analytics.....	27
3.3.2.1	Spectral properties	27
3.3.2.2	Thermal stability	28
3.3.2.3	Product formation.....	28
3.3.2.3.1	Substrate conversion on HMF, DFF and FFA	29
3.3.2.3.2	Product inhibition of FFA	29
3.3.2.4	Steady state kinetics of HFVW	30
3.4	Results.....	32
3.4.1	Site directed mutagenesis	32
3.4.2	Characterization of HMFO variants	32
3.4.2.1	Spectral properties and thermal stability.....	32
3.4.2.2	Product formation.....	33
3.4.2.2.1	Substrate conversion on HMF, DFF and FFA	33
3.4.2.2.2	Product inhibition of FFA	35
3.4.2.3	Steady state kinetics of HFVW	37
3.5	Discussion	41
3.5.1	Site directed mutagenesis	41
3.5.2	Characterization of HMFO variants	41
3.5.2.1	Spectral properties and thermal stability.....	42
3.5.2.2	Product formation.....	43
3.5.2.3	Steady state kinetics of HFVW	45
3.6	Conclusion and outlook	45
4	CHARACTERIZATION OF PUTATIVE L-AMINO ACID DEAMINASE	46
4.1	Introduction.....	46
4.1.1	Amino acids as chiral therapeutic drugs.....	46
4.1.2	L-amino acid deaminase from <i>Proteus myxofaciens</i>	46

4.2 Aim of work	47
4.3 Methods	48
4.3.1 Molecular biology procedures.....	48
4.3.1.1 Cloning LAAD variants.....	48
4.3.1.2 Cloning LAAD in pET-SUMO vector.....	50
4.3.1.3 Factors affecting (d)LAAD expression.....	52
4.3.1.3.1 Expression at different temperatures and shaking parameters.....	52
4.3.1.3.2 Alternative E. coli strains.....	53
4.3.1.4 Preparation of alditol oxidase.....	53
4.3.1.5 Purification of (d)LAAD.....	54
4.3.1.5.1 Expression for purification protocols.....	54
4.3.1.5.2 Purification protocol A.....	54
4.3.1.5.3 Purification protocol B.....	55
4.3.1.5.4 Purification protocol C.....	57
4.3.2 Analytics.....	58
4.3.2.1 Activity assays.....	58
4.3.2.2 Oxidase assay.....	58
4.3.2.3 Oxidoreductase assay.....	59
4.3.2.3.1 Redox dye testing.....	60
4.3.2.3.2 DCPIP oxidoreductase assay.....	61
4.3.2.4 Bradford assay.....	62
4.4 Results	63
4.4.1 Transmembrane helix prediction and LAAD variants design.....	63
4.4.2 Cloning LAAD variants.....	63
4.4.3 Cloning LAAD in pET-SUMO.....	65
4.4.4 Factors affecting (d)LAAD expression.....	65
4.4.4.1 Expression at different temperatures and shaking parameters.....	65
4.4.4.2 Alternative E. coli strains.....	66
4.4.5 Localization of dLAAD in the cell.....	67
4.4.6 Activity assays.....	70
4.4.6.1 Oxidase assay.....	70
4.4.6.2 Oxidoreductase assay.....	71
4.4.6.2.1 Redox dye testing.....	71
4.4.6.2.2 DCPIP oxidoreductase assay.....	72
4.5 Discussion	74
4.5.1 Cloning LAAD variants.....	74
4.5.2 Factors affecting (d)LAAD expression.....	74
4.5.3 Localization of dLAAD in the cell.....	75

4.5.4	Activity assays	75
4.6	Conclusion and outlook	76
5	ABBREVIATIONS	77
6	REFERENCES	80

1 Introduction

1.1 Flavin-dependent enzymes

Flavin-dependent enzymes, so called flavoenzymes, are ubiquitous enzymes. They are involved in a wide range of different type of reactions and play a big role in biological processes. They catalyze important reactions in physiological metabolisms, biosynthesis of metabolites and other cellular activities. Their outstanding chemical versatility lies in the flavin-based cofactor(s) and its reactivity towards inert molecules such as oxygen. [1] The reduction of oxygen can often generate toxic products, therefore is a tight control over oxygen in related reactions vital. [2]

Since the discovery of the first flavoenzyme in the 1930s [1], the number of discovered enzymes are progressively raising and further studied intensively.

Flavoenzymes can be found in multiple enzyme classes or families [3]. A vast majority of around 90 % belong to the enzyme class (EC) 1, the oxidoreductases. The rest are distributed over the transferases (EC 2), lyases (EC 4), isomerases (EC 5), and ligases (EC 6). [4]

Flavoenzymes are gaining interest in biocatalysis. Their unique combination of properties of selectivity and efficiency allow for a widespread use for industrial applications, drug discovery and synthesis. [5]

1.2 Flavin-based cofactors FAD and FMN

The characteristic yellow chromophore flavin gets its name from the Latin word *flavus* for its color. The cofactor flavin originates from the vitamin riboflavin and contains an isoalloxazine ring. This tricyclic ring system with its N1, C4a, N5 and C10a atoms forms the chemical and catalytical active center of the flavin structure and is depicted below in Figure 1-1. [6] [7]

The extraordinary ability of the conjugated double-bond system of the isoalloxazine ring allows for a typically stepwise transfer of up to two electrons to other compounds. Therefore, flavin has multiple redox states: an oxidized, a semi-quinone (one electron reduced) and a fully reduced hydroquinone (two electrons reduced) form. [8]

A flavoenzyme uses two half reactions to complete the transfer of both electrons, resulting in a reductive and oxidative half reaction cycle. First the flavin is reduced by an electron donor in the reductive half reaction. After the two electron transfers, the flavin later regenerates its oxidized state by an electron acceptor in the oxidative half reaction. [6] [8] [9]

The two most common derivatives of riboflavin are: flavin adenine dinucleotide (FAD) and flavin mononucleotide (FMN). FAD is the more common coenzyme with 75 % [4]. The structures of flavin-based cofactors are shown in Figure 1-1.

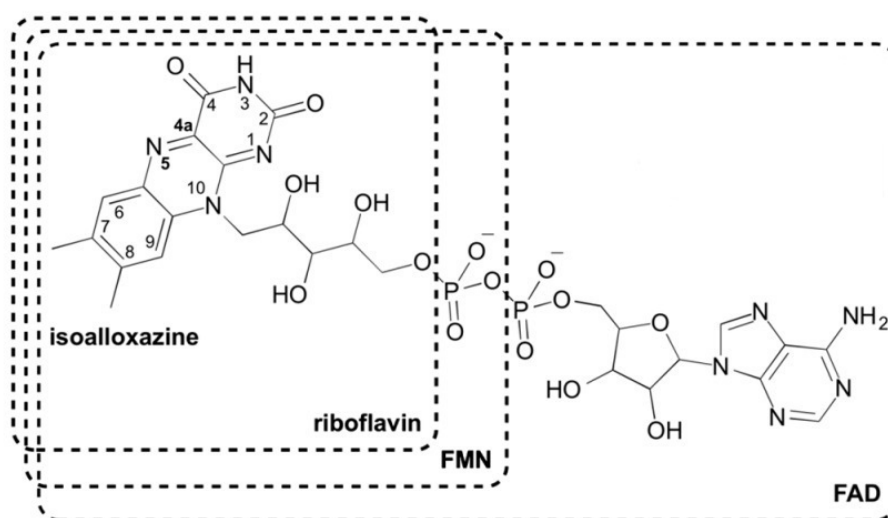


Figure 1-1 Chemical structures of flavin-based cofactors riboflavin, FMN and FAD. Adapted illustration from [8]. *FAD flavin adenine dinucleotide, FMN flavin mononucleotide*

Based on the redox state shown in Figure 1-2, FAD shows different chemically and spectroscopic properties. Each form shows a typical absorption spectrum that can be used for analysis. The oxidized form FAD has the highest absorption peak at a wavelength of 450 nm. [10] [11]



Figure 1-2 The oxidized FAD, semiquinone FADH and reduced FADH₂ form of flavin adenine dinucleotide. [10] *FAD flavin adenine dinucleotide*

1.3 HMF oxidase and L-amino acid deaminase

In this work two flavoenzymes were studied: HMF oxidase and L-amino acid deaminase. Both enzymes contain FAD as a coenzyme and show big potential for industrial application regarding their catalyzed reaction.

2 Materials

If not mentioned otherwise, below indicated materials were used for both projects. Materials used for only one project are specifically mentioned.

2.1 List of chemicals

2,5-Furandicarboxaldehyde $\geq 97\%$	Sigma-Aldrich (St. Louis, USA)
2,5-Furandicarboxylic acid 97%	Sigma-Aldrich (St. Louis, USA)
2,6-Dichlorophenol-indophenol	Sigma-Aldrich (St. Louis, USA)
3',3'',5',5''-Tetrabromophenol sulfonephthalein	Sigma-Aldrich (St. Louis, USA)
3,5-Dichloro-2-hydroxybenzenesulfonic acid sodium salt 99%	Sigma-Aldrich (St. Louis, USA)
4-Aminoantipyrine	Sigma-Aldrich (St. Louis, USA)
Acetic acid	Sigma-Aldrich (St. Louis, USA)
Ammonium persulfate	Sigma-Aldrich (St. Louis, USA)
4-Hydroxy-3-methoxybenzyl alcohol	Sigma-Aldrich (St. Louis, USA)
4-Hydroxy-3-methoxybenzaldehyde	Sigma-Aldrich (St. Louis, USA)
5-Formyl-2-furancarboxylic acid $>98\%$	Tokyo Chemical Industry (Tokyo, Japan)
5-Hydroxymethylfurfural $>99\%$	Sigma-Aldrich (St. Louis, USA)
Acetonitrile, HPLC Gradient Grade	Boom B.V. (Meppel, Netherlands)
Acrylamide	Sigma-Aldrich (St. Louis, USA)
Ampicillin sodium salt	Sigma-Aldrich (St. Louis, USA)
Agar, granulated	BD Biosciences (Franklin Lakes, USA)
Agarose MP, multipurpose	Sigma-Aldrich (St. Louis, USA)
Benzyl alcohol analytical standard	Sigma-Aldrich (St. Louis, USA)
Benzaldehyde $>99.5\%$	Sigma-Aldrich (St. Louis, USA)
Boric acid	Sigma-Aldrich (St. Louis, USA)
Bovine Serum Albumin, purified	New England Biolabs (Ipswich, USA)
Bradford Reagent	Sigma-Aldrich (St. Louis, USA)
Calcium chloride $\geq 93\%$	Sigma-Aldrich (St. Louis, USA)
ddH ₂ O	in-house
D-(+)-Glucose	E. Merck KG (Darmstadt, Germany)

Di-Potassium hydrogen phosphate	E. Merck KG (Darmstadt, Germany)
Dideuterio(phenyl)methanol 98% D	Sigma-Aldrich (St. Louis, USA)
Ethylenediaminetetraacetic acid	Sigma-Aldrich (St. Louis, USA)
Ethanol 70%, 96.2%	Boom B.V. (Meppel, Netherlands)
Flavin adenine dinucleotide disodium salt hydrate $\geq 95\%$	Sigma-Aldrich (St. Louis, USA)
Glycerol 85%	Boom B.V. (Meppel, Netherlands)
Hydrogen chloride	Sigma-Aldrich (St. Louis, USA)
Hydrogen peroxide	Sigma-Aldrich (St. Louis, USA)
InstantBlue™	Expedeon (Cambridge, UK)
Imidazole	Thermo Fisher Scientific (Waltham, USA)
Isopropyl- β -D-thiogalactoside	Sigma-Aldrich (St. Louis, USA)
Kaliumcyanide	Sigma-Aldrich (St. Louis, USA)
Kanamycin sulfate	Sigma-Aldrich (St. Louis, USA)
L-(+)-arabinose $\geq 99\%$	Sigma-Aldrich (St. Louis, USA)
L-phenylalanine $\geq 98\%$	Sigma-Aldrich (St. Louis, USA)
Magnesium sulfate	Sigma-Aldrich (St. Louis, USA)
Methylene blue	Sigma-Aldrich (St. Louis, USA)
Methylene green zinc chloride double salt	Sigma-Aldrich (St. Louis, USA)
MilliQ®	
N,N,N',N'-Tetramethylethylenediamine 99%	Sigma-Aldrich (St. Louis, USA)
N'N'-bis-methylene-acrylamide	Sigma-Aldrich (St. Louis, USA)
Ni-Sepharose resin	GE Healthcare Life Sciences (Chicago, USA)
Sodium azide	Sigma-Aldrich (St. Louis, USA)
Sodium chloride	E. Merck KG (Darmstadt, Germany)
Sodium dodecyl sulfate 98%	Sigma-Aldrich (St. Louis, USA)
Riboflavin 5'-adenosine diphosphate disodium salt $\geq 95\%$	Sigma-Aldrich (St. Louis, USA)
Phenylpyruvic acid 98%	Sigma-Aldrich (St. Louis, USA)
Potassium dihydrogen phosphate	E. Merck KG (Darmstadt, Germany)
Tris(hydroxymethyl)aminomethane	Sigma-Aldrich (St. Louis, USA)

Triton X-100	BDH Laboratory Supplies (Dorset, UK)
Tryptone	BD Biosciences (Franklin Lakes, USA)
Xylitol ≥99%	Sigma-Aldrich (St. Louis, USA)
Yeast Extract	BD Biosciences (Franklin Lakes, USA)

2.2 Buffers, gels and gel markers

Buffer

Potassium Phosphate buffer	12 mM / 50 mM/ 100 mM, pH 6.6 / 7 / 7.5 / 8
50 mM Tris/HCl buffer	50 mM Tris, adjusting pH with HCl, pH 7.5
50 mM Tris/HCl 150 mM NaCl buffer	50 mM Tris, adjusting pH with HCl, 150 mM NaCl pH 8

Gel buffer

1x Tris/Borate/EDTA buffer	89 M Tris, 89 M boric acid, 2 mM EDTA, pH 8
Stacking buffer 4x	0.5 M Tris/HCl pH 6.8, 0.4% (w/v) SDS
Resolving buffer 4x	1.5 M Tris/HCl pH 8.8, 0.4% (w/v) SDS

Purification buffers *HMFO project*

Standard buffer	50 mM Tris/HCl 150 mM NaCl pH 7.5
Lysis buffer	50 mM Tris/HCl 150 mM NaCl pH 7.5, 100 μM FAD, 10 % (v/v) glycerol
Imidazole buffer E500	50 mM Tris/HCl 150 mM NaCl pH 7.5, 500 mM imidazole
Imidazole buffer E50	50 mM Tris/HCl 150 mM NaCl pH 7.5, 50 mM imidazole
Imidazole buffer W10	50 mM Tris/HCl 150 mM NaCl pH 7.5, 10 mM imidazole
Imidazole buffer W5	50 mM Tris/HCl 150 mM NaCl pH 7.5,

5 mM imidazole

Gels

Mini-PROTEAN® Electrophoresis System	Bio-Rad Laboratories, Inc. (Hercules, USA)
Stacking gel 4%	30% Acrylamide/ N'N'-bis-methylene-acrylamide solution, 4x stacking buffer, MilliQ, 10% ammonium persulfate, N,N,N',N'-tetramethylethyldiamine
Resolving gel 9%/ 12%	30% Acrylamide/ N'N'-bis-methylene-acrylamide solution, 4x resolving buffer, MilliQ, 10% ammonium persulfate, N,N,N',N'-tetramethylethyldiamine

Gel markers

GelPilot DNA Loading Dye, 5x	QIAGEN N.V. (Venlo, Netherlands)
SmartLadder	Eurogentec (Seraing, Belgium)
PageRuler™ Prestained Protein Ladder	Thermo Fisher Scientific (Waltham, USA)
SDS Loading Buffer 2x	65.8 mM Tris/HCl pH 6.8, 2.1% SDS, 26.3% (w/v) glycerol, 0.01% 3',3'',5',5''- tetrabromophenolsulfonephthalein

2.3 Microorganisms*Escherichia coli*

BL21(DE3)	F ⁻ <i>ompT gal dcm lon hsdS_B</i> (r _B ⁻ m _B ⁻)	New England Biolabs (Ipswich, USA)
	λ (DE3 [<i>lacI lacUV5-T7p07 ind1 sam7 nin5</i>]) [<i>malB</i> ⁺] _{K-12} (λ ^S)	
C41(DE3)	F ⁻ <i>ompT gal dcm hsdS_B</i> (r _B ⁻ m _B ⁻) (DE3)	Lucigen Corporation (Wisconsin, USA)

C43(DE3)	F ⁻ <i>ompT gal dcm hsdS_B (r_B⁻ m_B⁻)</i> (DE3)	Lucigen Corporation (Wisconsin, USA)
TOP 10	F ⁻ <i>mcrA Δ(mrr-hsdRMS-mcrBC)</i> <i>φ80/lacZΔM15 ΔlacX74 nupG recA1</i> <i>araD139 Δ(ara-leu)7697 galE15</i> <i>galK16 rpsL(Str^R) endA1 λ⁻</i>	Invitrogen Corporation (Carlsbad, USA)

2.4 Plasmids

pET-SUMO	<i>E. coli</i> expression vector, TA cloning, T7 <i>lac</i> promoter, IPTG inducible, pBR322 origin, f1 origin, <i>lacI</i> , N-terminal 6xHis-tag, N-terminal SUMO-tag, kanamycin resistance	Invitrogen Corporation (Carlsbad, USA)
pET-21a(+)	<i>E. coli</i> expression vector, restriction cloning, T7 <i>lac</i> promoter, IPTG inducible pBR322 origin, f1 origin, <i>lacI</i> , T7 terminator, N-terminal T7-tag, optional C-terminal His-tag, multiple cloning site, ampicillin resistance	EMD Biosciences, Inc. (Madison, USA)
pBAD-MBP	pBADNdel-derived <i>E. coli</i> expression vector, <i>malE</i> gene and factor Xa protease cleavage site from pMALc2x inserted, <i>araBAD</i> promoter, L-arabinose inducible, pBR322 origin, C-terminal <i>c-myc</i> epitope and His-tag, ampicillin resistance	provided by M. Fraaije, University of Groningen

2.5 Enzymes

Alditol oxidase	provided by M. Fraaije, University of Groningen
<i>Taq</i> DNA polymerase 5 U/ μ L with <i>Taq</i> reaction buffer 10x	New England Biolabs (Ipswich, USA)
T4 Polynucleotide kinase 10 U/ μ L with T4 ligase buffer 10x	New England Biolabs (Ipswich, USA)
T4 Quick ligase 2 U/ μ L with T4 ligase buffer 10x	New England Biolabs (Ipswich, USA)
T4 DNA ligase 4 Weiss units/ μ L	Invitrogen Corporation (Carlsbad, USA)
SUMO protease 1 U/ μ L	Invitrogen Corporation (Carlsbad, USA)
<i>PfuUltra</i> II Fusion HS DNA polymerase	<i>PfuUltra</i> II Hotstart PCR Master Mix
<i>DpnI</i> 20 U/ μ L with NEBuffer VI 10x	New England Biolabs (Ipswich, USA)
Deoxyribonuclease I from bovine pancreas 400-800 U/mg	Sigma-Aldrich (St. Louis, USA)
Antarctic phosphatase 5 U/ μ L with Antarctic phosphatase reaction buffer 10x	New England Biolabs (Ipswich, USA)
Glucose oxidase from <i>Aspergillus niger</i> ≥ 100 U/mg	Sigma-Aldrich (St. Louis, USA)
Peroxidase from horseradish Type I 50-150 U/mg	Sigma-Aldrich (St. Louis, USA)
dATP 100 mM	New England Biolabs (Ipswich, USA)

Restriction enzymes were purchased from New England Biolabs (Ipswich, USA). PCR Primers were bought from Eurofins Scientific (Luxemburg, Luxemburg). Sequencing was performed by GATC Biotech AG (Constance, Germany).

2.6 Kits

High Pure Plasmid Isolation Kit Ref. 11754785001, Version 09	Roche Diagnostics International AG (Rotkreuz, Switzerland)
Expand™ Long Range dNTPack Ref. 04829034001, Version 06	Roche Diagnostics International AG (Rotkreuz, Switzerland)
QIAquick PCR Purification Kit Cat No./I.D. 28106	QIAGEN N.V. (Venlo, Netherlands)
Champion™ pET SUMO Expression System	Invitrogen Corporation (Carlsbad, USA)
<i>PfuUltra</i> II Hotstart PCR Master Mix	Agilent Technologies (Santa Clara, USA)
Ni Sepharose High Performance resin	GE Healthcare Life Sciences (Chicago, USA)

2.7 Instruments

Pipettes

Pipetman® Pipette P2, P10, P20, P100, P200, P1000, P5000	Gilson, Inc. (Middleton, USA)
Pipetman® Diamond Tips D10, DL10, D200, D300, D1000, D5000	Gilson, Inc. (Middleton, USA)
Pipette Refilltips Optifit 100 µL, 200 µL, 350 µL, 1000 µL	Sartorius Biohit Liquid Handling Oy (Helsinki, Finland)
Picus mLINE® Single Channel Pipet 120 µL, 300 µL, 5000 µL	Sartorius Biohit Liquid Handling Oy (Helsinki, Finland)
Picus mLINE® Multichannel Electronic Pipet 10 µL, 100 µL, 5000 µL	Sartorius Biohit Liquid Handling Oy (Helsinki, Finland)
Picus mLINE® Multichannel Mechanical Pipet 10 µL, 100 µL, 300 µL	Sartorius Biohit Liquid Handling Oy (Helsinki, Finland)

Flasks, tubes, syringes and needles

DURAN® Erlenmeyer flask various volumes	DWK Life Sciences GmbH (Mainz, Germany)
DURAN® laboratory bottle various volumes	DWK Life Sciences GmbH (Mainz, Germany)
Sapphire PCR tube 0.5 mL	Greiner Bio-One GmbH (Frickenhausen, Germany)
Biosphere® SafeSeal reaction tube 1.5 mL	Sarstedt (Nuembrecht, Germany)
Eppendorf® safe lock tubes 2.0 mL	Eppendorf AG (Hamburg, Germany)
Eppendorf® tubes 5.0 mL	Eppendorf AG (Hamburg, Germany)
CELLSTAR® centrifuge tubes 15 mL, 50 mL, (non-) skirted	Greiner Bio-One GmbH (Frickenhausen, Germany)
Terumo™ three-part syringe 2 mL, 5 mL, 10 mL, 20 mL	Terumo Europe (Leuven, Belgium)
Sterican® single-use hypodermic needle Ø 0.8 mm x 120 mm	B.Braun Melsungen AG (Melsungen, Germany)
NORM-JECT® two-part syringe 1 mL	Henke-Sass Wolf (Tuttlingen, Germany)
BRAND® standard disposable cuvettes	BRAND GMBH + CO KG (Wertheim, Germany)
Econo-Pac® 10DG Desalting Column	Bio-Rad Laboratories, Inc. (Hercules, USA)
Econo-Pac® Chromatography Column 20 mL	Bio-Rad Laboratories, Inc. (Hercules, USA)

Centrifugation

Microcentrifuge Heraeus™ Fresco™ 17	Thermo Fisher Scientific (Waltham, USA)
Centrifuge 5424	Eppendorf AG (Hamburg, Germany)
Avanti™ J-E High performance centrifuge rotors JA17, JA14, JLA-10.500	Beckman Coulter, Inc. (Brea, USA)

Centrifuge 5810R
rotors A-4-62-MTP, F-34-6-38
Eppendorf AG (Hamburg, Germany)

PCR

peqSTAR 96 Universal Gradient
Isogen Life Science B.V
(De Meern, Netherlands)
CFX96 Touch™ Real-Time PCR System
Bio-Rad Laboratories, Inc.
C1000 Touch Thermal cycler
(Hercules, USA)
Mastercycler personal
Eppendorf AG (Hamburg, Germany)

HPLC *HMFO project*

Solvent mixing module HG-980-31
Jasco (Easton, USA)
Autosampler AS-1555
Jasco (Easton, USA)
Ternary gradient unit LG-980-02S
Jasco (Easton, USA)
UV/Vis detector UV-2075Plus
Jasco (Easton, USA)
Pump PU-980
Jasco (Easton, USA)
Multiwave detector MD-910
Jasco (Easton, USA)
Software LC-Net II/ADC
Jasco (Easton, USA)
Column Zorbax Eclipse XD8-C8 5µm
Agilent Technologies
(Santa Clara, USA)

Spectrophotometry

UV/Vis Spectrophotometer
Jasco Deutschland GmbH
V-650, V-660
(Pfungstadt, Germany)
Vis Spectrophotometer
Jenway (Staffordshire, UK)
Jenway 6300
Multi-mode reader microplate reader
BioTEK Instruments, Inc.
Synergy Mx
(Winooski, USA)
NanoDrop™ 1000 Spectrophotometer
Thermo Fisher Scientific
(Waltham, USA)

O₂ measurements

Optical Oxygen Meter FireStingO₂
Pyroscience (Aachen, Germany)
REDFlash Sensor spots
Pyroscience (Aachen, Germany)

GraphPad software	GraphPad Software, Inc. (La Jolla, USA)
Miscellaneous	
Bunsenburner	
Whatman™ Filter 0.2 µM	GE Healthcare Life Sciences (Pittsburgh, USA)
ThermoMixer® C 1.5 mL, 2.0 mL	Eppendorf AG (Hamburg, Germany)
ThermoMixer® Comfort 1.5 mL	Eppendorf AG (Hamburg, Germany)
Vortex shaker MIX TM01	Retsch (Haan, Germany)
Digital Dry Heat Block Heater	VMR (Radnor, USA)
Precision balance PRO 32/34F	Sartorius AG (Goettingen, Germany)
Analytical balance MC1 LC480UP	Sartorius AG (Goettingen, Germany)
Analytical balance AG245	Mettler-Toledo (Zurich, Switzerland)
Parafilm® M	Bemis Company (Neenah, USA)
Autoclave HST 6x7x9, LTA 2x3x4	Zirbus Technology (Bad Grund, Germany)
Incubator shaker Innova 44, Innova 4430	New Brunswick Scientific (Edison, USA)
Incubator IN55	MemMert GmbH +Co. KG (Schwabach, Germany)
Sonicator Virba-cells Processor VCX 130	Sonics & Materials, Inc. (Newtown, USA)
Orbital shaker OS-40	Lab4you GmbH (Berlin, Germany)
Professional pH Meter PP-25	Sartorius AG (Goettingen, Germany)
Purifier® Class II Biosafety Cabinet	Labconco Corporation (Kansas City, USA)

3 Structure-function analysis of HMF oxidase

3.1 Introduction

3.1.1 FDCA and HMF as building blocks for new polymers

In the face of steadily growing awareness of climate change, the demand for replacement of fossil oil-based products such as plastic is posing a big global challenge. [12] Biomass as a renewable raw material and alternative carbon source represents a promising way into the future. [13]

2,5-Furandicarboxylic acid is ranked as one of the top twelve of value-added renewable chemicals from biomass [14]. It serves as the building block of a wide variety of polymers. FDCA can be derived from abundant hexose sugars like fructose and glucose. Polymerized with ethylene glycol, it provides the base for a new kind of plastic: Polyethylene furanoate. This bio-based polyester is on its way to replace the familiar and commonly used polyethylene terephthalate (PET) plastic. [15]

PEF has a highly improved gas barrier performance that extends the shelf life of products. Furthermore, it shows similar mechanical properties compared to oil-derived PET. [16]

FDCA can be synthesized through a chemical cascade starting from sugar derivative 5-hydroxymethylfurfural. In a first acid catalyzed dehydration step the hexose derivatives are turned into HMF. In traditional chemical processes, production of HMF and the following oxidations to FDCA are done with strong oxidants or metal-salt catalyzers. Those reactions happen under various combinations of harsh conditions such as under high pressure (up to 70 bar) or temperatures (up to 180°C) and can take a long time (up to 48 hours). [16] [17]

HMF can also be directly oxidized to FDCA using enzymes. Enzymes provide for a unique environment in which they catalyze most chemical conversions at room temperature and atmospheric pressure [18].

The recently described flavoenzyme HMF oxidase can catalyze the full conversion of HMF in three consecutive steps. This is remarkable, because so far this was just accomplished using several and different enzymes. [19]

3.1.2 The oxidation pathway of HMF to FDCA by HMF oxidase

The formation of FDCA by HMFO involves three consecutive oxidation steps and is shown in Figure 3-1. Every step is a two-electron oxidation which consumes one equivalent of oxygen (O_2) and forms one equivalent of hydrogen peroxide (H_2O_2).

The first oxidation is initiated by a conserved histidine active site residue (H467) of HMFO. The removal and transfer of a proton of the alcohol group of HMF to FAD results in the formation of 2,5-furandicarboxaldehyde (DFF). In the process FAD gets reduced and in a side reaction reoxidized by molecular O_2 producing H_2O_2 . The second step leads to the formation of 5-formyl-2-furancarboxylic acid (FFA) by oxidizing the aldehyde group of hydrated DFF. Finally, hydrated FFA is converted to FDCA. [20] [21] [22]

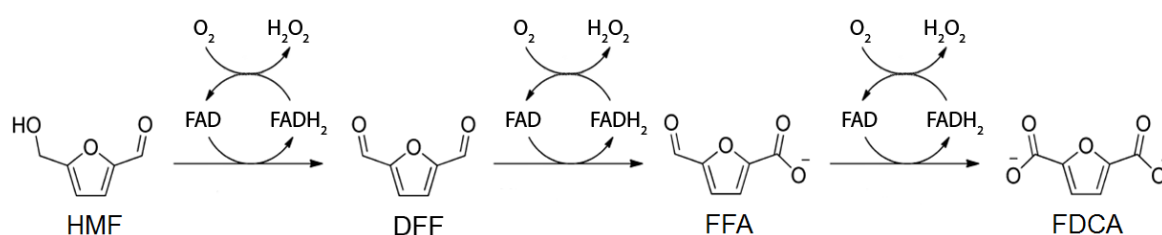


Figure 3-1 Oxidation pathway involving HMF, DFF, FFA and FDCA by HMFO.

Adapted illustration from [22]. *DFF* 2,5-furandicarboxaldehyde, *FAD* flavin adenine dinucleotide, *FADH₂* reduced form of flavin adenine dinucleotide, *FDCA* 2,5-furandicarboxylic acid, *FFA* 5-formyl-2-furancarboxylic acid, *HMF* 5-hydroxymethylfurfural, *H₂O* water, *H₂O₂* hydrogen peroxide, *O₂* oxygen

Up to this date no other enzyme can perform all necessary oxidation steps on its own [20] [23]. HMFO acts on alcohol (HMF), aldehyde (DFF) and hydrated aldehyde (FFA) groups.

3.1.3 HMF oxidase

The bacterium *Cupriavidus basilensis* was known to be capable of growing with HMF as its sole carbon source using the HMF oxidoreductase HmfH (UniProtKB entry D5KB61). When HmfH was expressed in the bacterium *Pseudomonas putida* a complete oxidation of HMF into FDCA became possible. [19]

As of today, purification and subsequent characterization of HmfH has not succeeded. A homology search of HmfH led to the discovery of an enzyme with a 46% amino acid (aa) sequence identity: HMF oxidase from *Methylovorus sp.* strain MP688. As HmfH, HMFO is involved in the oxidation pathway from HMF to FDCA. [20]

Escherichia coli (*E. coli*) is a valuable and proven host for industrial applications [24] and was therefore the choice of host. A synthetic, for *E. coli* codon optimized *hmfo* gene was used. So, HMFO could be overexpressed and purified to apparent homogeneity. [20]

HMFO is a flavin-dependent oxidase (EC 1.1.3.47; UniProtKB entry E4QP00) and belongs to the glucose-methanol-choline family of oxidoreductases [25]. The enzyme consists of 531 aa and has a molecular weight of 70.4 kDa. The pH optimum lies at pH 8 and the temperature optimum at 55°C. So, reactions between 20 and 70°C are possible. The enzyme relies on a not covalently bound FAD cofactor. [20] The crystal structure of HMFO (PDB entry 4UDP in oxidized state, 4UDQ in reduced state) with bound FAD was solved. HMFO forms a monomeric globular structure with two domains: a cofactor binding domain and a smaller cap domain that covers the flavin site. [22]

3.1.4 Limitations in current HMF oxidase catalyzed FDCA production

The rate limiting step with HMFO lies in the final oxidation of FFA to FDCA and no complete conversion takes place. This is due to a high affinity for FFA ($K_M > 4$ mM) for the wildtype (WT) enzyme.

A comparison of the crystal structure of HMFO and a model based on the sequence of HmfH regarding the substrate binding in the active site was made. Multiple residues of interest were identified in a preliminary study by W. Dijkman, PhD from the University of Groningen, Netherlands.

Four single mutations turned out to be of most interest for enhancing the FFA affinity. This thesis focused on the exchange of four special amino acids of HMFO: H333M, F352Y, V367R, W466F. The crystal structure of HMFO with the mutations positions can be seen in Figure 3-2. [20]

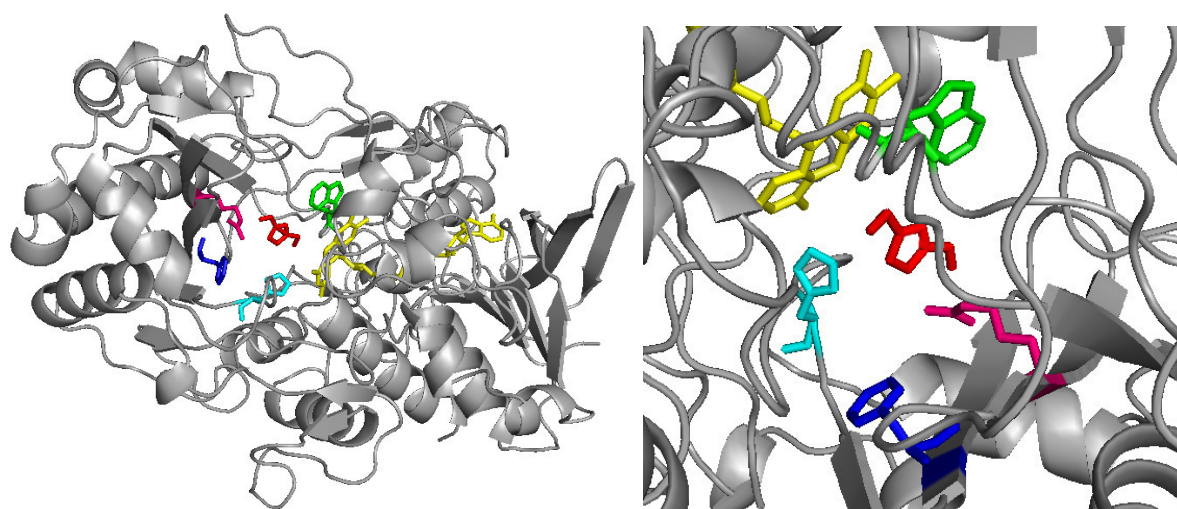


Figure 3-2 Crystal structure of mutated HMFO with modelled bound HMF substrate in the active site cavity. Ribbon diagram of overall structure with colored mutations and cofactor FAD bound. HMF in red, FAD in yellow, H333M in cyan, F352Y in blue, V367R in pink, W466F in green. *FAD flavin adenine dinucleotide, HMF 5-hydroxymethylfurfural, HMFO HMF oxidase*

The amino acid position changes in 333 and 352 are directly linked to HmfH in the done structure comparison. These two homologous residues differed between HMFO and HmfH and both are in the area of potential influence of the substrate. Changing the polar histidine 333 to a non-polar methionine introduces a secondary methionine in the active site. The other methionine M103 in the same area helps keeping the necessary hydrophobic environment for the activity of HMFO, as an alternation was previously proven to lead to decreased activity [22]. The change of a non-polar residue phenylalanine 352 to a polar tyrosine should stabilize the carboxyl group of FFA. The positive charge of the arginine in V367R is to be believed to stabilize the negatively charged carboxyl group of FFA. Near the active site base H467, in the conserved position W466 a tryptophan is changed for a less spacious phenylalanine. This gives HMF more space to position itself in the binding cavity.

In this thesis, these single variants and variations thereof were studied in detail:

single variants	H333M (H), F352Y (F), V367R (V), W466F (W)
double variants	H333M/F352Y (HF), V367R/W466F (VW)
quadruple variant	H333M/F352Y/V367R/W466F (HFVW)

3.2 Aim of work

The objective of this work was to improve the catalysis of HMF of the HMFO wildtype enzyme in *E. coli*. The focus should be on the last rate limiting step of FDCA formation. Therefore, the construction of HMFO variants based on structure-function analysis were necessary.

To achieve this objective, various aims were defined:

1. Creation, cloning and expression of four selected single and three combined multiple HMFO variants
2. Purification of the wildtype and HMFO variants to apparent homogeneity for characterization
3. Basic characterization of obtained enzymes with respect to thermal stability and spectral properties
4. Determination of apparent kinetics parameters of the quadruple variant
5. Conversion experiments and product pattern analysis

3.3 Methods

3.3.1 Molecular biology procedures

3.3.1.1 *Media preparation*

3.3.1.1.1 *Lysogeny broth medium*

Lysogeny broth medium (LB) was used for standard molecular procedures such as cultivation, transformation, storing and freezing *E. coli*. The medium consisted of 10 g/L tryptone, 10 g/L sodium chloride (NaCl), and 5 g/L yeast extract in double distilled water (ddH₂O). For preparing LB agar plates 15 g/L LB agar was added. The solution was autoclaved at 121°C for 20 min. If needed, filter sterilized final 50 mg/L kanamycin or ampicillin antibiotic was added after cooling down to handling temperature. The medium was stored at 4°C.

3.3.1.1.2 *Terrific broth medium*

Terrific broth medium (TB) was used for expression of protein in *E. coli*. This growth medium contained 24 g/L yeast extract, 12 g/L tryptone and 4 mL/L glycerol dissolved in ddH₂O. A salt solution of 2.31 g/L potassium dihydrogen phosphate and 16.43 g/L dipotassium hydrogen phosphate in ddH₂O was autoclaved separately and added aseptically before inoculation. Both solutions were autoclaved at 121°C for 20 min. After cooling down to handling temperature, filter sterilized final 50 mg/L kanamycin or ampicillin was added. The medium was stored at 4°C.

3.3.1.2 *Determination of cell density*

The optical density (OD₆₀₀) of *E. coli* cells was measured at 600 nm with a visible spectrum (Vis) spectrophotometer Jenway 6300. OD₆₀₀ measurements allow for an estimation of cell concentration in diluted suspensions [26]. Medium or buffer of an experiment was used as reference. Samples were diluted with medium or buffer to a maximum OD₆₀₀ of 0.9.

3.3.1.3 Production of *E. coli* competent cells

E. coli competent cells for heat shock transformation were made by calcium chloride (CaCl₂) treatment [27].

50 mL of sterile LB in a sterile 250 mL flask were inoculated with 1:100 of an overnight preculture (ONC) of *E. coli* cells from stock in LB medium without antibiotic. After an OD₆₀₀ of 0.5 was reached the cells were centrifuged (15 min, 4000 rpm, 4°C, swingout centrifuge) and the pellet was resuspended carefully in 20 mL sterile on-ice-kept 0.1 M CaCl₂ solution. Subsequently the cells were incubated for 15 min on ice and centrifuged down as before. Resuspension of the pellet was done in 3 mL on-ice-kept 0.1 M CaCl₂ and 1 mL 50% volume per volume (v/v) glycerol in 0.1 M CaCl₂. After 15 min incubation on ice 110 µL aliquots were made, frozen in liquid nitrogen and stored at -80°C.

3.3.1.4 Heat shock transformation

Transformations necessary for protein expression experiments were made with *E. coli* BL21(DE3) cells and for all other transformations *E. coli* TOP 10 cells were used. A test transformation with a positive (plasmid) and negative (without plasmid) control was carried out in later performed transformations.

Except for pET-SUMO based plasmids which were transformed exactly as described in [28], plasmid transformations were carried out as described briefly in the following.

Plasmid deoxyribonucleic acid (DNA) transformations were performed by heat shock treatment. [29] Therefore 50 µL on-ice-kept calcium-competent cells and 10 - 100 ng of plasmid DNA were mixed in a sterile 1.5 mL tube and incubated for 20 min on ice. The cells were heat shocked in a heat block at 42°C for 30 - 60 s, followed by cooling them for 1 min on ice. 450 µL LB medium without antibiotic was added and the cells recovered (30 min to 1 h, 37°C). The cells were spun down, resuspended in 50 - 250 µL LB medium and 50 - 250 µL plated on LB-agar containing kanamycin or ampicillin. The plates were incubated at 37°C overnight (o/n) and colonies counted the next day. For further experiments the plates were stored at 4°C.

3.3.1.5 PCR product purification

For polymerase chain reaction (PCR) product purification the QIAquick PCR Purification Kit was used. The purification steps were followed according to the manual. To increase the DNA concentration, the incubation temperature and time before elution were 37°C and 5 min, respectively instead of the manufacturer's recommended settings.

3.3.1.6 Plasmid isolation and purification

The plasmid isolation and purification were carried out with the High Pure Plasmid Isolation Kit and the standard protocol as recommended by the manufacturer was applied.

3.3.1.7 Site directed mutagenesis

To introduce mutations into HMFO (EC 1.1.3.47; UniProtKB entry E4QP00), a pET-SUMO vector carrying the wildtype *hmfo* gene [20] fused to a His-SUMO-tag was used as a template [28]. The template and a list with potential active site mutations in HMFO were kindly provided by W. Dijkman, PhD from the University of Groningen, Netherlands.

For enhancing the product yield, four mutations from the provided list were chosen. The mutations were selected based on prior carried out docking experiments by W. Dijkman and modelling of substrate binding in the HMFO active site using the program YASARA [30] described in [22].

Multiple variants and variants combinations were introduced using a mutant strand synthesis PCR followed by *DpnI* digestion [31]. In the PCR the whole plasmid was copied and the mutations introduced with specific primers.

First four single mutants were produced: H, F, V and W. Two single mutants (H and V) were used as template to introduce another mutation (F or W), creating the two double variants HF and VW. Based on double mutant HF, two single mutations (V and W) were added to create a quadruple variant HFVW.

In Table 3-1 the forward and reverse primer for each single mutant are listed.

Table 3-1 PCR primer for single variants in HMFO.

primer	sequence from 5'end to 3'end
H333M forward	GTAAAGCCGGCTCTCGCATGCAACTGGGTATCCGTGC
H333M reverse	GCACGGATACCCAGTTGCATGCGAGAGCCGGCTTTAC
F352Y forward	CGATATGCAGATACAGGTCTAGGCGTCGC
F352Y reverse	GCGACGCCTAGCGACCTGTATCTGCATATCG
V367R forward	GGCTTGTTACCCAGAAACGAGCGCTTGCCAGACCGC
V367R reverse	GCGGTCTGGCAAGCGCTCGTTTCTGGGTGAACAAGCC
W466F forward	CCGCTCGCATGGAAAACACCGCCGACGTTTCGT
W466F reverse	ACGAACGTGGCGGTGTTTTCCATGCGAGCGG

For the PCR the *PfuUltra* II Hotstart PCR Master Mix was used. The altered PCR reaction set-up and temperature profile are shown in Table 3-2 and Table 3-3. The PCR products were purified and eluted in 40 μ L heated elution buffer.

Table 3-2 PCR reaction for single mutations in HMFO.

component	volume [μ L]
2 x Mastermix <i>Pfu</i> Hotstart (buffer, enzyme, dNTPs, Mg ²⁺)	10
10 μ M forward primer	0.5
10 μ M reverse primer	0.5
100 ng pET-His-SUMO-HMFO	x
MilliQ	to end volume of 20

Table 3-3 Temperature profile of PCR reaction for single mutations in HMFO.

PCR step	time [min]	temperature [°C]	
initial denaturation	5	95	
denaturation	0.5	95	} 18x
annealing	1	55	
extension	11	72	
final extension	20	72	
store	∞	4	

First all single variants were created. The second round of mutations were introduced afterwards with the corresponding second set of primers. The quadruple mutant was made by using the double mutant HF as a template for introducing the other two mutations in two consecutive PCRs.

Non-methylated template DNA was specifically digested through the addition of *DpnI*. In Table 3-4 the *DpnI* digestion set-up is listed. The *DpnI* digestion of the PCR product was carried out for 1.5 to 2 h at 37°C.

Table 3-4 *DpnI* digestion set-up.

component	volume [µL]
purified PCR product	20
NEB buffer IV	2.2
<i>DpnI</i>	0.5

Afterwards purification of the DNA was performed and eluted in 30 to 40 µL heated elution buffer. The DNA concentration was measured using the Nanodrop spectrophotometer and an agarose gel 0.8% was run to check for availability of plasmid.

Further around 100 ng eluted plasmid was transformed to competent *E. coli* TOP10 cells. Transformed cells were plated on LB-kanamycin plates, cultivated o/n at 37°C and stored at 4°C. Single colonies from these master plates were inoculated individually in 5 mL LB-kanamycin o/n at 37°C. On the next day the plasmids were

isolated from *E. coli* TOP10 cells and send for sequencing using either pET-SUMO forward or TEV (tobacco etch virus) reverse primers. Variants V, W, VW and HFVW were fully sequenced [20] [32]. In H, F and HF the mutated region was sequenced.

3.3.1.8 Expression

For HMFO(-variants) expression the pET-His-SUMO-HMFO plasmid (with or without mutations) was transformed into *E. coli* BL21(DE3). An o/n culture was diluted 1:100 in TB medium with 50 µg/mL kanamycin and grown (37°C, 200 rpm) to an OD₆₀₀ of 0.5. Cells were induced at room temperature with filter-sterilized isopropyl-β-D-thiogalactoside (IPTG) at a final concentration of 1 mM and further cultivated at 17°C and 180 rpm for 68 h.

Cell concentrations were determined by OD₆₀₀ measuring before the cells were spun down by centrifugation (JLA 14 rotor, 6000 g, 4°C, 15 min). The cells were stored at -20°C for further experiments.

3.3.1.9 Purification

Purification of HMFO(-variants) involved sonification, immobilized metal ion affinity chromatography, desalting and sodium dodecyl sulfate polyacrylamide gel electrophoresis (SDS-PAGE) analysis. Samples along all purification steps were taken for SDS-PAGE gel analysis.

The harvested and frozen *E. coli* BL21(DE3) cell pellets (of a 100 mL culture with an OD₆₀₀ of 16 to 20) containing HMFO were carefully resuspended in 30 mL lysis buffer in weighted 50 mL Greiner tubes and samples were pooled if necessary. The cells in the 50 mL Greiner tubes were disrupted by sonification (see section 3.3.1.13). The cell lysate was spun down (JLA 17 rotor, 15 000 g, 4°C, 1 h).

Gravity-flow chromatography was used for purification of HMFO from the cell-free extract in a Nickel (Ni) Sepharose resin column. The with nickel-precharged, crosslinked sepharose beads had a binding capacity of 40 mg bound enzyme/mL resin. The needed volume of the resin column (CV) was determined based on the expected enzyme mass (20 mg enzyme per 100 ml cell culture) and the double CV of resin beads was used. The resin beads were mixed 1:1 with 70% ethanol, put on the bottom of a 20 mL chromatography column and the ethanol was drained. The set

beads were rinsed with 5 CV of MilliQ and 7 CV of a solution containing 50 mM tris(hydroxymethyl)aminomethane/hydrogen chloride (Tris/HCl), pH 7.5 and 150 mM NaCl.

The soluble, cell-free extract fraction was incubated (1 to 2 h, 4°C, 50 rpm) with prepared Ni Sepharose resin in a 50 mL Greiner tube. After spinning down the resin (2x 1 min, 4°C, 800 rpm), the pellet was resuspended in 5 CV standard buffer and the suspension put in a 20 mL chromatography column.

In a series of alternating washing (using 3 CV of W5 and W10) and elution steps (using 3 CV of E50 and E500) all fractions were collected in 1.5 mL tubes. The individual fractions were collected manually as concentrated as possible depending on the color intensity of the eluate. A 3 mL 10DG desalting column was prepared by draining the sodium azide in which it was stored, rinsing the column with 10 mL MilliQ followed by 10 mL 50 mM Tris/HCl buffer pH 7.5. The eluates were pooled and 3 mL of eluate desalted with 4.5 mL 50 mM Tris/HCl buffer pH 7.5 using a prepared 10 DG desalting column. For a new desalting round the column was rinsed with 10 mL 50 mM Tris/HCl buffer pH 7.5.

The yellow desalted fractions were pooled, analyzed and stored with glycerol at -80°C. The molar extinction coefficient and concentration of the protein fraction was determined before storing. The efficiency of the purification process was analyzed by SDS-PAGE gel electrophoresis using the taken samples after each step.

3.3.1.10 *Gel electrophoresis*

For all gel electrophoresis experiments the Mini-PROTEAN Electrophoresis system was used.

3.3.1.11 *Agarose gel electrophoresis*

Agarose gel electrophoresis was performed for identification of DNA products. In general, 0.8% weight per volume (w/v) gels were used. 1x Tris/Borate/EDTA buffer was chosen as running buffer and for good band separation the gel was run at 82 V for around 30 min. As standard for size identification the SmartLadder was used.

3.3.1.12 SDS-PAGE gel electrophoresis

For protein identification SDS-PAGE gel analysis was done. 9 or 12% SDS gels were prepared and run at 200 V for around 45 min. All samples were mixed with 20 μ L 2x SDS-Loading Dye in 1.5 mL tubes, heat deactivated (5 min, 80°C) and spun down (5 min, room temperature, 21 000 g). The gels were stained (o/n, room temperature, 100 rpm) with 3x InstantBlue. For use as size standards the PageRuler™ Prestained Protein Ladder was applied.

For the LAAD project thawed LAAD pellets were resuspended in 50 μ L 50 mM Tris/HCl buffer pH 7.5 containing 150 mM NaCl.

3.3.1.13 Sonication

Preparation of cell lysates from *E. coli* were done by sonication. Cells were lysed by liquid shear forces and cavitation through applying ultrasonic frequencies. [33]

Sonication was performed with a Sonicator Virba-cells processor VCX 130. Probe sizes were chosen depending on the sample volume. During sonication the cells were kept on ice and the probe was positioned in the center of the cell lysate.

For the HMFO project cells were sonicated in 50 mL Greiner tubes. The cell suspension was sonicated with 10 s on/ 20 s off cycles for 10 min at 50% amplitude.

For the LAAD project cells were sonicated in 1.5 or 2 mL tubes. The cell suspension was sonicated with 2 s on/ 2 s off cycles for 1 min at 50% amplitude.

3.3.2 Analytics

3.3.2.1 *Spectral properties*

The cofactor FAD is bound not covalently to HMFO and gets released upon denaturation of the enzyme. Unbound FAD shows fluorescent activity. Therefore, resulting in a typical FAD absorbance spectrum with an absorbance maximum. [20] By measuring the absorption of free and enzyme-bound FAD and using the law of Lambert-Beer the enzyme concentration and the molar extinction coefficient of the enzyme-bound FAD could be calculated [34] [35].

The ultraviolet–visible (UV/Vis) spectrum of free and HMFO-bound FAD was recorded (25°C, 200 nm/min, 0.5 nm intervals) in two measurements with a Jasco PAC-743R spectrometer between 250 and 600 nm. In the first absorption measurement the concentrated purified enzyme was diluted 1:10 with 50 mM Tris/HCl buffer pH 7.5 and the bound FAD absorption measured. For the second measurement the enzyme buffer solution was mixed with SDS to a final concentration of 0.1% (w/v) and incubated for 5 min at room temperature. During the SDS treatment the enzyme unfolded and the subsequent spectrum was that of free FAD.

With the measured UV/Vis spectrum of free and HMFO-bound FAD, the spectral properties were calculated using the law of Lambert-Beer in Equation 1.

In Equation 1, A_λ stands for absorption at wavelength λ , ϵ_λ for molar extinction coefficient of the FAD-bound enzyme at wavelength λ [$\text{mM}^{-1}\text{cm}^{-1}$], c for concentration of enzyme solution [mM] and d for distance of the light path [cm]. The distance of the light path refers to the length of the used cuvette and was set at 1 cm.

$$A_\lambda = \epsilon_\lambda * c * d \quad \text{Equation 1}$$

The molar ratio of HMFO-bound-FAD is equal to HMFO-freed-FAD. The molar extinction coefficient of purchased FAD at 450 nm was known to be $11.3 \text{ mM}^{-1}\text{cm}^{-1}$ [20]. By measuring the absorption of HMFO-freed-FAD at 450 nm an estimated concentration of enzyme could be calculated using the law of Lambert-Beer. When the enzyme concentration was known, the FAD-bound enzyme molar extinction coefficient

could be determined by again using the law of Lambert-Beer. The wavelength with the absorbance according to the determined ϵ_{λ} was read out. [34] [35]

3.3.2.2 *Thermal stability*

To determine the thermal stability of HMFO(-variants) the ThermoFAD method was applied [36]. This method is a variation of the ThermoFluor method [37] specifically designed for flavoproteins. Accordingly, the FAD fluorescence increase was measured upon FAD release from the unfolding enzyme due to temperature increase. [36]

The melting temperature of the enzyme was measured in double measurements in a real-time PCR. 10 μ M purified enzyme was diluted 1:10 in 50 mM Tris/HCl buffer pH 7.5 and a temperature gradient in 0.5°C steps from 20 to 90°C was used.

3.3.2.3 *Product formation*

Analysis of substrate conversion from the HMFO variants was carried out by reversed phase high performance liquid chromatography (HPLC) with UV detection [38]. HMFO converts HMF to FDCA via two intermediates, DFF and FFA. All four compounds were separated by a Zorbax Eclipse XDB-C8 5 μ m column as a hydrophobic stationary phase. A 12 mM potassium phosphate buffer (KPi) pH 7.0 and organic solvent acetonitrile were used as eluent. The gradient profile of the mobile phase can be seen in Table 3-5.

Table 3-5 HMFO HPLC gradient profile.

time [min]	12 mM potassium phosphate buffer pH 7.0 [%]	acetonitrile [%]
1	100	0
4.5	95	5
7	60	40
7.5	60	40
8	100	0
10	100	0

The HPLC set up can be found in section 2.7 and further parameters are listed in Table 3-6.

Table 3-6 HMFO HPLC parameters.

parameter	units
flowrate	1.2 mL/min
pressure	0-25 mPA
detection	268 nm
sample volume	10 μ L
method time	10 min

The expected retention times with this setup were 1.2 min for FDCA, 1.8 min for FAA, 6 min for DFF and 6.4 min for HMF.

Calibration curves were done for all compounds in a range from 0.1 to 2 mM compound dissolved in 100 mM KPi buffer pH 7.0.

3.3.2.3.1 *Substrate conversion on HMF, DFF and FFA*

Each step of the conversion of HMF to FDCA, starting with HMF, DFF or FFA respectively, was carried out separately with each of the 7 variants and the WT.

For all three conversion steps 20 μ M of purified enzyme and 5 mM substrate were used. All reactions were carried out in 100 mM KPi buffer pH 7.0 in 70 μ L reaction volume (25°C, 1000 rpm). The reactions were stopped after 2 h by heat inactivation (5 min, 70°C). Inactivated reaction mixtures were centrifuged (5 min, 13 000 g) and supernatant diluted 1:10 with 100 mM KPi buffer pH 7.0 before HPLC analysis. Reactions under identical conditions but without enzyme were carried out as negative controls to correct for any resulting spontaneous autooxidation of substrates.

3.3.2.3.2 *Product inhibition of FFA*

To investigate a possible substrate inhibition at high FFA concentrations, five 1:3 dilution steps starting with 33 mM to 0.14 mM FFA concentrations were tested with a fixed amount of 5 μ M enzyme. All single mutants, double mutant HF and the WT were tested in 100 mM KPi buffer pH 7.0 in 100 μ L reaction volume (25°C, 1000 rpm). The reaction was stopped after 1 and 2 h by heat deactivation (5 min, 70°C) and

centrifuged (5 min, 13 000 g). The samples were analyzed undiluted by HPLC. Autooxidation samples (FFA and buffer solution) were performed along as well. A FFA calibration curve was done with the same dilution steps.

3.3.2.4 Steady state kinetics of HFVW

The apparent kinetic parameters of the quadruple variant HFVW were investigated by monitoring O₂ consumption during catalysis. So, a comparison of this data with the WT, single mutant V and the double mutant VW from literature [20] [22] were possible. The oxygen decrease was measured with precalibrated REDFLASH sensor spots (100% saturation equaled 268 μM O₂), a Firesting O₂ fiber-optic oxygen meter and a light source. The REDFLASH sensor spots are working based on an oxygen sensitive dye under red-orange light excitation. This dye has a quenching effect on O₂. Its luminescence in the near infrared increases with decreasing oxygen. [39]

All reactions were performed with HMF, DFF and FFA as substrate in a 50 mM KPi buffer pH 8.0 at 25°C at atmospheric oxygen concentration. The reaction volume was 500 μL and substrates were applied in a range of final 0 μM to 40 mM while 2.5 μM HFVW were used. The enzyme concentration was stable throughout the complete reaction. Experiments were done in duplicates.

The oxygen sensor was placed into the reaction mixture and the oxygen level recorded for one minute before the reaction was initiated by the addition of enzyme.

The reaction was monitored for about two minutes. Reference experiments were conducted under exactly the same conditions but leaving out substrate or enzyme.

The initial rates were determined by following the oxygen level decrease [%] over time [s]. Using Microsoft Excel, a slope was generated out of the linear part of the data set. The resulting %/s measurements had to be converted to μM/s using the precalibrated standard measurement of 1% oxygen is 2.68 μM. One mole of oxygen utilized corresponds in accordance to the stoichiometry of the reaction to one mole of substrate converted.

Dividing the oxygen decrease rate [μM/s] by the enzyme concentration gave the initial reaction rate [s⁻¹] at a given substrate concentration. The given slope was corrected for the 0 μM substrate blank reference measurement.

The calculated initial rates at given substrate concentrations were curve fitted with the Michaelis–Menten kinetics equation (for HMF) (see Equation 2) or an equation considering substrate inhibition (for DFF and FFA) (see Equation 3) using GraphPad to estimate the apparent kinetic parameters. The determined apparent kinetic parameters were the maximum enzyme velocity (V_{max}) and the Michaelis-Menten constant (K_M). The turnover number (k_{cat}) equaled V_{max} .

In Equation 2, v stands for initial rate of the enzyme, V_{max} for the maximum enzyme velocity [s^{-1}], X for substrate concentration [mM], K_M for Michaelis-Menten constant [mM].

In Equation 3, v refers to the initial rate of the enzyme, V_{max} to the maximum enzyme velocity [s^{-1}], X to the substrate concentration [mM], K_M to the Michaelis-Menten constant [mM] and K_I to the dissociation constant for substrate binding [mM].

$$v = \frac{V_{max} * X}{K_M + X} \quad \text{Equation 2}$$

$$v = \frac{V_{max} * X}{K_M + X * \left(\frac{1 + X}{K_I}\right)} \quad \text{Equation 3}$$

The catalytic efficiency (k_{cat}/K_M) was determined by dividing k_{cat} by K_M .

3.4 Results

3.4.1 Site directed mutagenesis

PCR amplifications using the template pET-SUMO-HMFO with mutation-specific primers produced single PCR products. By sequencing, the introduction of the desired mutations could be proven. Successful PCR constructs were achieved for all seven variants of HMFO: H, F, HF, V, W, VW and HFVW. All pET-SUMO-HMFO variants were successfully transformed and expressed in *E. coli*.

3.4.2 Characterization of HMFO variants

3.4.2.1 *Spectral properties and thermal stability*

The apparent melting temperature T_m and the spectral properties including the FAD-bound enzyme molar extinction coefficient ϵ_{max} and wavelengths λ of absorption maxima A_{max} , were determined for the WT and all HMFO variants. Results are summarized in Table 3-7.

The WT had a T_m of 47.5°C. The variants F and HF showed an increased T_m by three to four degrees. V, W and VW were not as stable as the WT and had lower melting temperatures (45°C, 43°C and 41°C). The quadruple variant, having the favourable VW mutation, had a 3.5°C higher T_m than the VW double mutant.

The comparison of the spectral properties of all variants were not displaying big variations, except for a higher ϵ_{max} of W and HFVW.

Table 3-7 Spectral properties and thermal stability of HMFO WT and variants. T_m apparent melting temperature, λ wavelengths of absorption maxima A_{max} , ϵ_{max} FAD-bound enzyme molar extinction coefficient

	WT	H	F	HF	V	W	VW	HFVW
T_m [°C]	47.5	47.5	50.5	51.5	45	43	41	44.5
λ of A_{max} [nm]	456	454.5	455	457	456	449	449	448.5
ϵ_{max} [mM ⁻¹ cm ⁻¹]	10.7	10.8	11.4	11	11.4	13.4	11.3	12.5

3.4.2.2 Product formation

To attain more insight into the impact of mutations in HMFO, the conversion of HMF and its derivatives was monitored over time. Oxidation of HMF to FDCA is carried out by HMFO via the two intermediates DFF and FFA. Starting the oxidation reaction at DFF results in a DFF, FFA and FDCA product pattern. Respectively, a start at FFA shows a pattern consisting out of FFA and FDCA.

3.4.2.2.1 Substrate conversion on HMF, DFF and FFA

The reactions were started by adding a fixed amount of 5 mM of HMF, DFF or FFA to a fixed amount of 20 μ M of enzyme. After termination of the reaction after 2 h, all samples were analyzed by HPLC with respect to the products formed. All reactions were performed with the wildtype and the seven variants of HMFO: H, F, HF, V, W, VW and HFVW.

Conversion results with HMF, DFF or FFA as substrates are depicted in Figure 3-3, Figure 3-4 and Figure 3-5, respectively. Due to extensive use of the Zorbax Eclipse XDB-C8 5 μ m column a full separation between HMF and DFF was not possible anymore.

Results in Figure 3-3 show a complete conversion of HMF and DFF to FFA and FDCA in the case of the WT and variants H, F, W and HF. Their FFA yield lay between 74 and 87%. Interestingly, variants VW and HFVW converted HMF or DFF less efficiently

into FDCA with HMF/DFE yields of around 50 and 65%. A significant difference was apparent in variant V with the best FDCA yield of 68% of all variants.

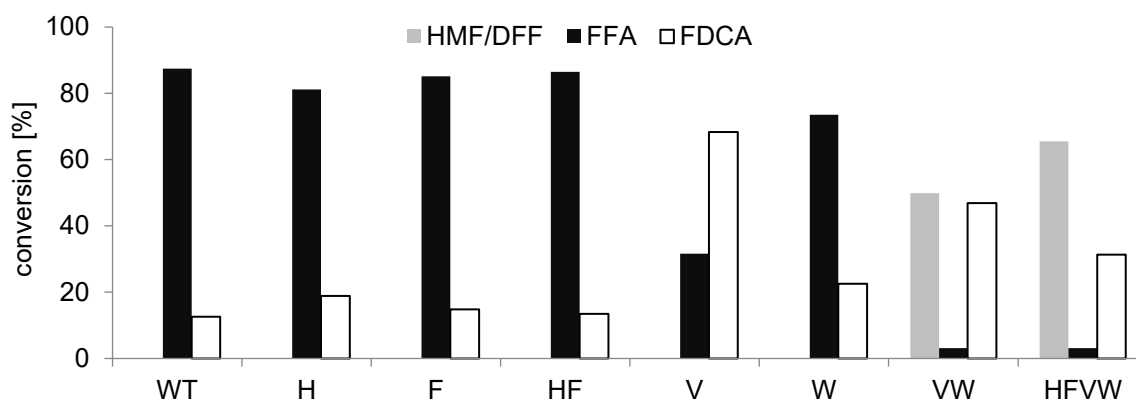


Figure 3-3 Product pattern of 20 μ M of all HMFO variants starting on 5 mM HMF after 2 h. 100% conversion means the substrate is completely converted. HMF and DFE were not clearly separated by the column anymore and are displayed as one. *DFE 2,5-furandicarboxaldehyde, FDCA 2,5-furandicarboxylic acid, FFA 5-formyl-2-furancarboxylic acid, HMF 5-hydroxymethylfurfural*

Figure 3-4 results give a similar product pattern starting on DFE as on HMF, showing up to 10% slightly higher FDCA levels across V, W, VW and HFVW.

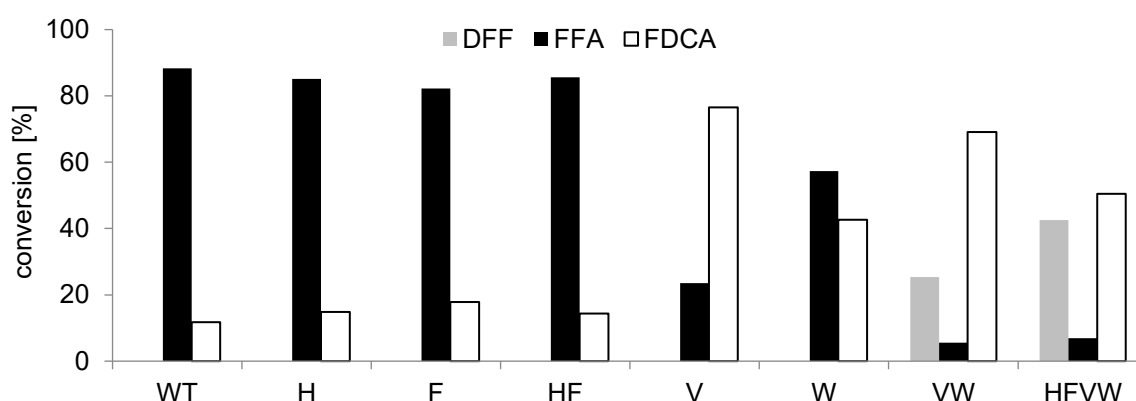


Figure 3-4 Product pattern of 20 μ M of all HMFO variants starting on 5 mM DFE after 2 h. 100% conversion means the substrate is completely converted. *DFE 2,5-furandicarboxaldehyde, FDCA 2,5-furandicarboxylic acid, FFA 5-formyl-2-furancarboxylic acid*

Figure 3-5 depicts with around 12 to 23% FDCA yield a low conversion of FFA to FDCA in WT, H, F and HF. Variants V, VW and HFVW displayed the highest FDCA yields of 86 to 96% starting on FFA.

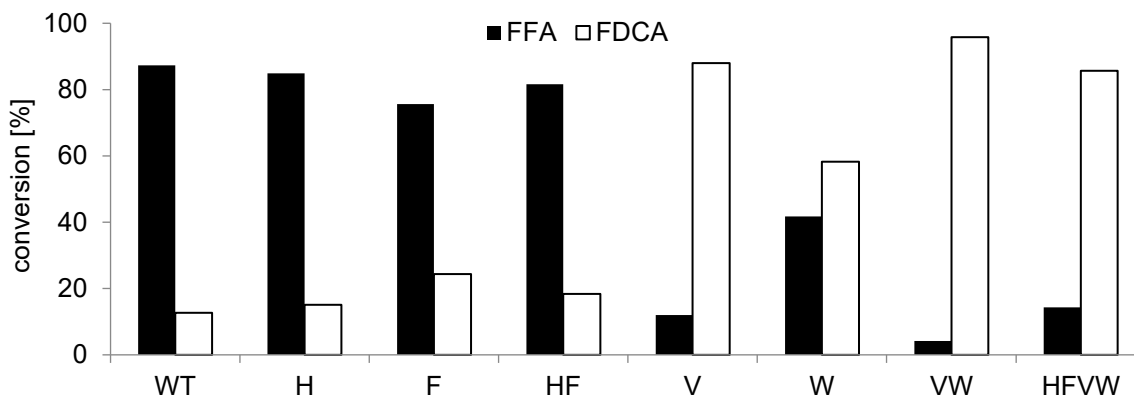


Figure 3-5 Product pattern of 20 μ M of all HMFO variants starting on 5 mM FFA after 2 h. 100% conversion means the substrate is completely converted. *FDCA* 2,5-furandicarboxylic acid, *FFA* 5-formyl-2-furancarboxylic acid

3.4.2.2.2 Product inhibition of FFA

To determine a possible substrate inhibition of FFA, a range of FFA concentrations was tested with a defined amount of 5 μ M enzyme. The conversions of different starting concentrations of FFA to FDCA after 1 and 2 h incubation were analyzed by HPLC. These reactions were done with the WT and five variants of HMFO: H, F, HF, V and W.

FDCA formed after 1 h can be seen in in Figure 3-6 and after 2 h in Figure 3-7, respectively. The WT and variants H, F and HF showed a constant product titer for FDCA concentrations larger than 3.5 mM. For V and W instead, product concentration levels decreased with increasing substrate concentrations, implying substrate inhibition.

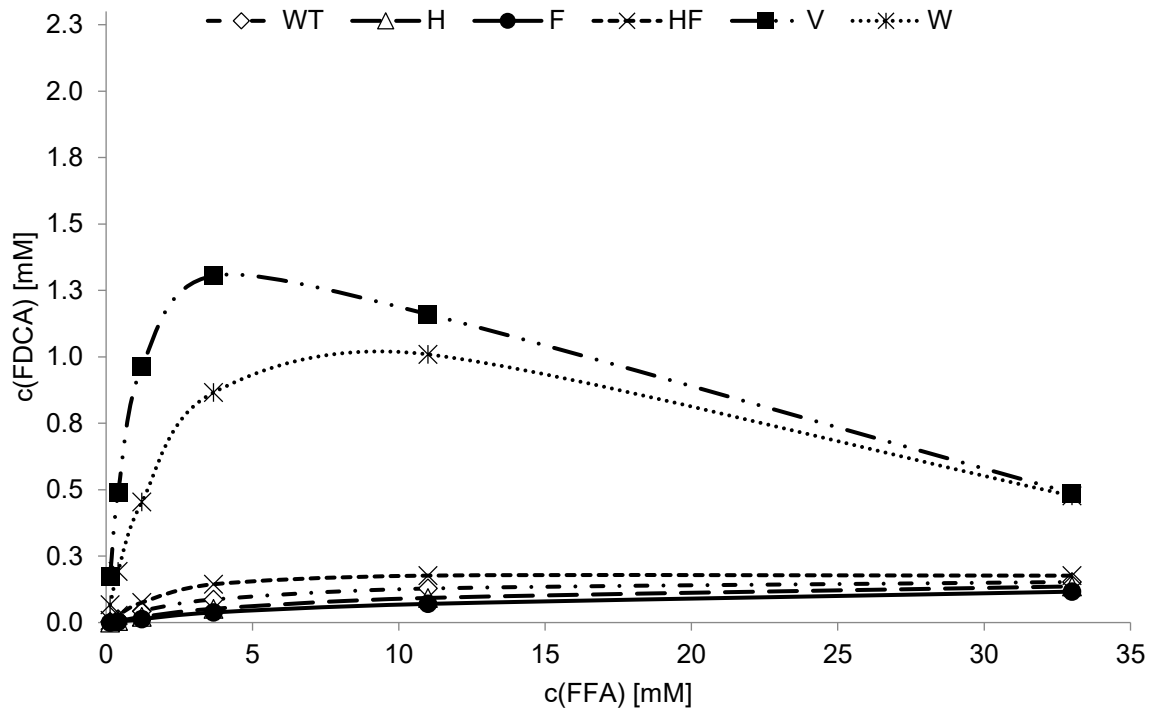


Figure 3-6 FDCA produced from FFA by 5 μ M of different HMFO variants after 1 h of incubation. FDCA 2,5-furandicarboxylic acid, FFA 5-formyl-2-furancarboxylic acid

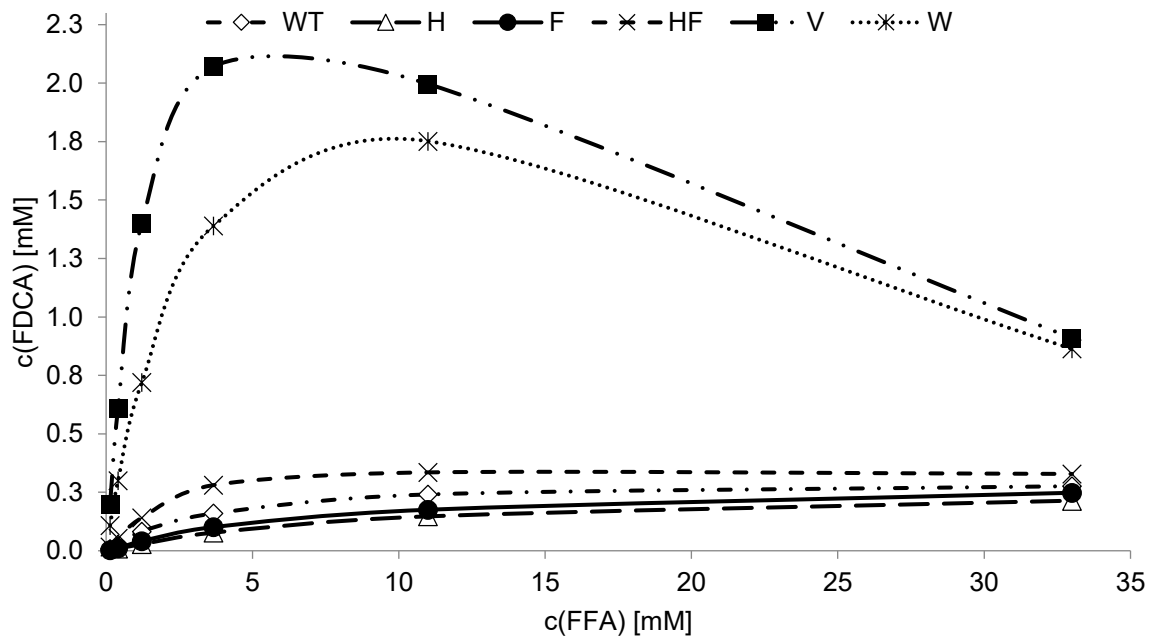


Figure 3-7 FDCA produced from FFA by 5 μ M of different HMFO variants after 2 h of incubation. FDCA 2,5-furandicarboxylic acid, FFA 5-formyl-2-furancarboxylic acid

3.4.2.3 Steady state kinetics of HFVW

The apparent kinetic parameters K_M , V_{max} and k_{cat} of HFVW were determined by following the O_2 decrease during catalysis. The reactions of a stable amount of 2.5 μM enzyme and a range of substrate concentrations HMF, DFF and FFA were monitored. Figure 3-8 summarizes the experimental data of initial rates plotted against the substrate concentrations. The initial rates of HFVW in plot B using DFF and in plot C using FFA as substrate are depicting a decline at higher concentrations. Remarkably in comparison with the WT, HFVW seemed to show a decline in the rates on DFF.

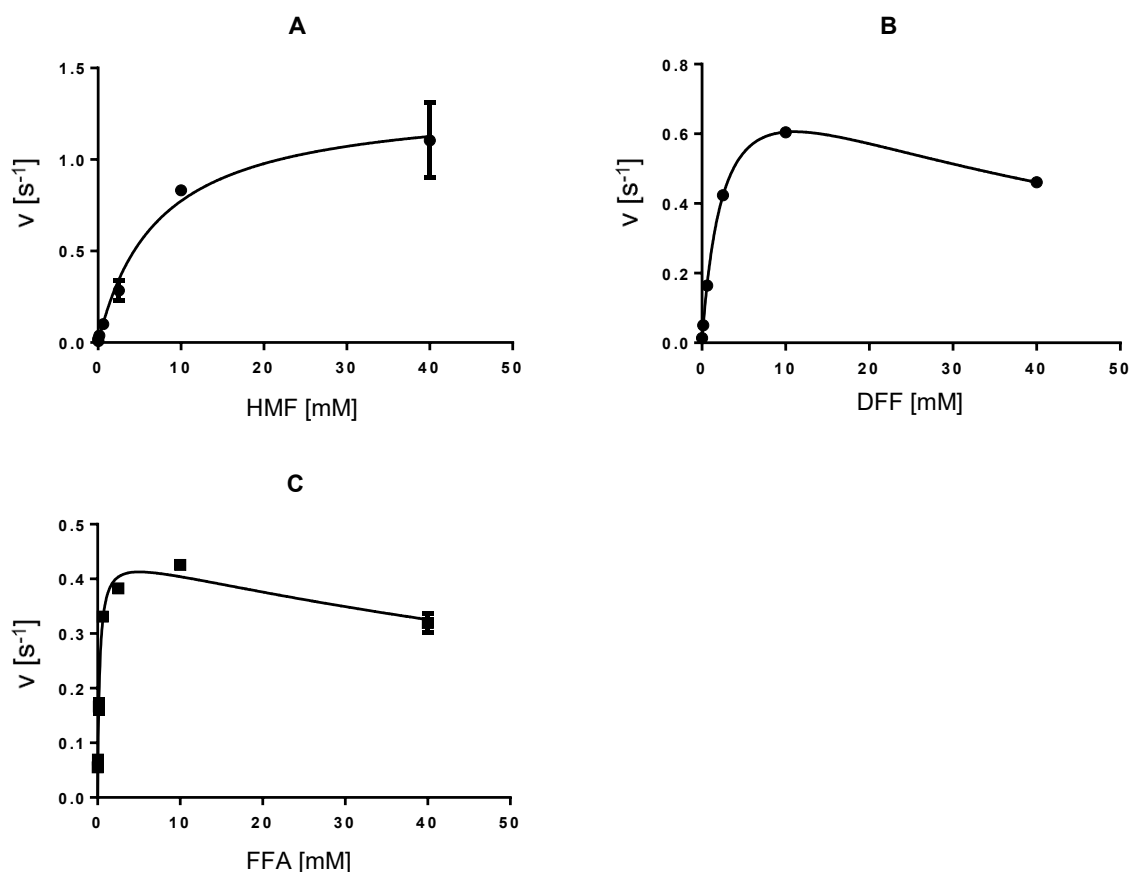


Figure 3-8 Plots of initial rates v and substrate concentrations for determination of apparent kinetic parameters of HFVW. Initial rates were determined at 25°C, 50 mM potassium phosphate buffer pH 8.0, using 2.5 μ M of purified enzyme and a range of 0 to 40 mM substrate. Data in A and B were fitted by Michaelis-Menten equation and Data in C by an equation considering substrate inhibition using GraphPad. **A** using HMF as substrate **B** using DFF as substrate **C** using FFA as substrate *DFF* 2,5-furandicarboxaldehyde, *FFA* 5-formyl-2-furancarboxylic acid, *HMF* 5-hydroxymethylfurfural

The resulting apparent kinetic parameters are listed in Table 3-8. HFVW showed the best k_{cat} with 0.45 s⁻¹ and highest affinity with the lowest K_M of 0.25 mM for FFA. Therefore, the best catalytic efficiency was also to be found for the same product. On the other hand, K_I was with 104 mM as well the highest for FFA compared to the other two substrates. An around 400 times higher K_I than K_M for FFA indicated a substantial loss of productivity. There was no substrate inhibition observed for HMF.

Table 3-8 Apparent kinetics parameters of HFVW on substrates HMF, DFF and FFA. Kinetic data of HFVW was measured at 25°C, 50 mM potassium phosphate buffer pH 8.0, using 2.5 µM of purified enzyme and a range of 0 - 40 mM substrate, apparent kinetics parameters were calculated using GraphPad. *DFF* 2,5-furandicarboxaldehyde, *FFA* 5-formyl-2-furancarboxylic acid, *HMF* 5-hydroxymethylfurfural, K_M Michaelis-Menten constant, k_{cat} turnover number, k_{cat}/K_M catalytic efficiency, K_I dissociation constant for substrate binding

	HMF	DFF	FFA
K_M	7.2	2.7	0.25
[mM]	± 1.5	± 0.1	± 0.04
k_{cat}	1.3	0.9	0.45
[s ⁻¹]	± 0.1	± 0.02	± 0.02
k_{cat}/K_M	0.185	0.331	1.84
[s ⁻¹ mM ⁻¹]			
K_I	-	44.4	104
[mM]		± 2.5	± 28

A comparison of HFVW data with data from literature from V, VW and WT and their respective apparent kinetic parameters on HMF and FFA were done. This comparison is to be seen in Table 3-9.

In comparison with WT, variants VW and HFVW displayed a big improvement for the K_M value of around 0.21 to 0.25 mM on FFA. Both variants in general showed the same apparent kinetics parameters on FFA.

In case of HMF as substrate V and WT indicated better k_{cat}/K_M values than HFVW.

Table 3-9 Apparent kinetics parameters comparison of HFVW on substrates HMF and FFA and WT, V and VW. HMF 5-hydroxymethylfurfural, FFA 5-formyl-2-furancarboxylic acid, K_M Michaelis-Menten constant, k_{cat} turnover number, k_{cat}/K_M catalytic efficiency

	HMF			FFA		
	K_M [mM]	k_{cat} [s ⁻¹]	k_{cat}/K_M [s ⁻¹ mM ⁻¹]	K_M [mM]	k_{cat} [s ⁻¹]	k_{cat}/K_M [s ⁻¹ mM ⁻¹]
WT ^{a)}	1.4	9.9	7.1	>4.0	-	-
V ^{a)}	0.7 ± 0.05	4.2 ± 0.1	6.2	1.4 ± 0.3	0.06 ± 0.004	0.041
VW ^{a)}	-	-	-	0.21 ± 0.07	0.46 ± 0.05	2.2
HFVW ^{b)}	7.2 ± 1.5	1.3 ± 0.1	0.185	0.25 ± 0.04	0.45 ± 0.02	1.8

a) data obtained from [20] and [22]

b) using data from Table 3-8

- not determined

3.5 Discussion

3.5.1 Site directed mutagenesis

A previously made list of potential interesting mutations by W. Dijkman [22] [20] and performed mutagenesis experiments were used to attain a deeper knowledge of the impact of several residues related to substrate conversion.

The four selected residues were: H333M, F352Y, V367R and W466F. H333M and F352Y were chosen because of their homology in the comparison of the enzyme structures of known HMF converting HmfH and HMFO. The other two mutation positions were selected on basis of their chemical and stereotypical properties in regard to important neighboring residues such as the substrate (V367R) and the active site base H467 (W466F).

The four single mutations were successfully combined to two double and one quadruple variant providing the ground work of the characterization of H, F, HF, V, W, VW and HFVW.

Variants V, W, VW and HFVW were fully sequenced [22] [32]. In H, F and HF the mutated region was sequenced.

The chosen pET-SUMO vector relies on a small ubiquitin-related modifier (SUMO) fused in front of the protein to enhance soluble expression. A N-terminal 6xpolyhistidine(His)-tag was fused to the protein for later protein purification [40]. So, up to 200 mg of HMFO(-variants) per liter *E. coli* BL21(DE) cell culture could be harvested after a cultivation period of 68 hours at 17°C and 180 rpm. The yellow color of the enzyme and it's His-tag made easy purification with immobilized metal ion affinity chromatography possible.

3.5.2 Characterization of HMFO variants

HMFO is the only reported and studied enzyme catalyzing the conversion of HMF to FDCA by itself. [20] This reaction of three oxidation steps relies on the oxidations of alcohols and aldehydes, which so far was just accomplished using several and different enzymes in a whole-cell biotransformation. [19]

The characterization of new variants led to better understanding of the structure-function relationship. Seven variants were studied and compared to the wildtype regarding their spectral properties, thermal stability and product formation. Furthermore, the Michalis-Menten parameters of the quadruple variant were determined.

3.5.2.1 Spectral properties and thermal stability

Using the UV/Vis absorption of free and enzyme-bound FAD and the law of Lambert-Beer the spectral properties of the variants could be calculated [34] [35]. The concentration of flavin-containing monomeric HMFO and of free flavin were equal. So, when these spectral properties are known, then the enzyme concentration can easily be estimated. In case of the enzyme extinction coefficient and wavelengths of absorption maxima no big differences were observed. All measured ϵ_{\max} and λ of A_{\max} values were within the range of those of the WT (ϵ_{\max} at $10.7 \text{ mM}^{-1}\text{cm}^{-1}$, A_{\max} at 456 nm), except for W and HFVW showing slightly higher ϵ_{\max} of 13.4 and $12.5 \text{ mM}^{-1}\text{cm}^{-1}$.

The thermal stability of the enzyme can be evaluated by its apparent melting temperature. The apparent melting temperatures were determined using the ThermoFAD method [36]. The temperature at the highest measured FAD fluorescence upon FAD release from the enzyme corresponds with the apparent melting temperature. The T_m of the wildtype lay at 47.5°C . The introduction of mutations had different impact on the thermal stability of the enzyme. The introduction of the mutation F352Y led to a significant increase of 3°C to 50.5°C in F. In contrast the V367R and W466F mutations led to a decrease by 2.5°C and even 4.5°C , respectively. This was reflected in the T_m s of the double and quadruple variants containing the mentioned single mutations. The negative impact of both single mutations V367R and W466F was to be seen in VW with the lowest temperature of 41°C . Whereas HF showed the highest T_m of all variants with 51°C , containing the benefitting mutation F352Y. HFVW had a T_m of 44.5°C . Both effects could be seen in HFVW: a better T_m than VW with a difference of 3.5°C , but a worse T_m compared to HF.

3.5.2.2 *Product formation*

The conversion of HMF to FDCA involves three distinct oxidations: HMF to DFF, DFF to FFA and finally FFA to FDCA [20]. In a first set of experiments, a step by step analysis of the three stages was done by starting each oxidation separately with the respective substrate. In a separate experiment the supposed substrate inhibition of FFA was examined.

The product analysis was done by reversed phase HPLC with UV detection [38]. In general, a 100% conversion meant the substrate was completely converted (into other products) and no substrate was detected by HPLC.

The product pattern of each oxidation step was studied with 20 μ M of all seven variants and the WT and 5 mM of substrate.

Independently of the substrate applied, similar levels of around 15% FDCA yield were obtained by the WT. Each time a complete turnover of the start substrates HMF and DMF took place, accumulating FFA and FDCA in the end. This resonated with a known low K_M value of 1.7 mM and a k_{cat}/K_M value of 7.1 s⁻¹mM⁻¹ on HMF and a high K_M (> 4 mM) on FFA from literature [22] [20].

Variants H, F and HF showed very similar product pattern as the wildtype. No matter the starting substrate, the final FDCA yield always lay beneath 23% and a complete HMF and DFF conversion was reached. The two single mutations H333M and F352Y had an almost neglectable effect on the product yield compared to the WT. The product pattern as well as the rate of catalysis were similar at the same enzyme concentration. It was therefore implied that both mutations might not be directly involved with substrate binding and catalysis.

In case of variants V, W, VW and HFVW, more complex and different product patterns were observed showing significantly higher FDCA yields (reaching up to 96%) across substrates. In general, the less oxidation steps needing to be performed by the variants, the higher the FDCA yield. The highest FDCA yields between 86 and 96% were measured in the FFA step. The best yields were achieved by variants VW with 96%, V with 88% and HFVW with 86%.

Surprisingly, beginning the oxidation reaction at HMF or DFF resulted in just partial conversion of both substrates in variants VW and HFVW. HMF and DFF levels were measured at the end of the stopped reaction. This was not observed for any single

variant. Due to the column, no clear distinction of HMF and DFF was possible and they were measured as one.

The high FDCA yields and the partial conversion of HMF/DFF of VW and HFVW were in accordance with their kinetic values determined in this work (HFVW) and from literature [22] (VW). Summarized, the high FDCA yields of over 86 % were reflected by similar low K_M s of 0.25 (VW) and 0.21 mM (HFVW). Better k_{cat}/K_M s of 1.8 (VW) and $2.2 \text{ s}^{-1}\text{mM}^{-1}$ (HFVW) on FFA were reported as well for both variants. They showed a high affinity for FFA. In contrast, a high K_M value of 7.2 mM and a very low k_{cat}/K_M value of $0.185 \text{ s}^{-1}\text{mM}^{-1}$ for HFVW on HMF was measured (no K_M or k_{cat}/K_M on FFA determined for VW). This reflected the low affinity for HMF and the partial conversion in the experiment.

The effect on FDCA production at FFA concentrations up to 40 mM were tested with 5 μM of all single mutants, HF and the WT.

The WT, H, F and HF showed a constant product titer for FDCA concentrations larger than 3.5 mM, thus implying no occurring substrate inhibition. In contrast, for V and W product concentration levels decreased with growing substrate concentrations. This suggested substrate inhibition.

Substrate inhibition in flavoenzymes is a well-known phenomenon. Partial or irreversible binding of the substrate to the flavin can result from the formation of added stable covalent bonds. [41]

Due to the introduction of V367R and W466F, these additional bonds seemed to cause the inhibition. From literature substrate inhibition was reported on FFA as well for V and VW with K_I values of 76 and 7.3 mM [22].

This poses a challenge for the future application of HMFO. It would be necessary to keep FFA concentrations at a tolerable minimum level for the whole duration of the production process to take full advantage of higher FDCA yields.

3.5.2.3 *Steady state kinetics of HFVW*

The steady state kinetics for the HFVW variant were determined by monitoring O₂ consumption and hence the substrate conversion during catalysis. All three oxidation steps were again investigated.

The calculated K_M , k_{cat} and k_{cat}/K_M values on the different substrates confirmed the product formation results, as already mentioned and discussed above.

K_I values of 44 and 104 mM were calculated in this work, for DFF and FFA respectively.

3.6 Conclusion and outlook

Since its introduction as a unique flavin oxidase, HMFO is a promising enzyme for the biocatalytic production of FDCA starting on HMF. So far fantastic improvements regarding to up to 96% FDCA yields with the introduction of the V367R and W466F mutations could already be achieved in this study. Furthermore, with H333M and F352Y two other important mutations for higher thermal stability were found.

Even though HMFO is still far away from being produced on industrial scale: the setting up of a biocatalytic reaction with the right host organism and an efficient downstream process for harvesting highly pure FDCA are challenges not yet even thought about. Nevertheless, if these challenges are overcome in the future HMFO could help make PEF an even cleaner alternative to PET compared to its traditional production [16].

4 Characterization of putative L-amino acid deaminase

4.1 Introduction

4.1.1 Amino acids as chiral therapeutic drugs

The importance of chirality in life regarding biological, chemical and physiological activity is omnipresent. If one or two compounds are non-superimposable mirror images of each other, they are called enantiomers. Each member of an enantiomer pair can show different properties and cause different effects. Except glycine, all amino acids are enantiomorph and have a chiral center. Consequently, they exist as enantiomers in a so-called L- or D- form.

The need for enantiomer selective and/or (highly) pure amino acids as chiral pharmaceutical intermediates or drugs is getting bigger in pharmaceutical and agricultural industry. Stereoselective enzymes can form an alternative to common low effective or more cost intensive separation methods for the production of enantiomeric compounds such as amino acids. [42]

4.1.2 L-amino acid deaminase from *Proteus myxofaciens*

The putative L-amino acid deaminase (LAAD) from bacterium *Proteus myxofaciens* is a very distinct enzyme. It is established that the enzyme is a membrane flavoenzyme, containing FAD as a cofactor. It consists out of 474 aa and has a molecular weight of around 51 kDa. The enzyme plays a role in the conversion of L- to D-amino acids. It converts L-amino acids into the corresponding α -keto acid and ammonia. This α -keto acid can then be further turned into D-amino acid using another enzyme. The catalyzed reaction by LAAD is shown in Figure 4-1. [43]

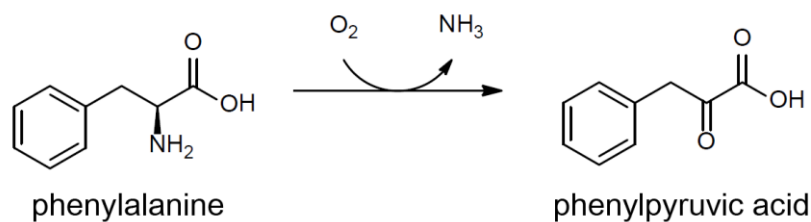


Figure 4-1 The oxidation of L-phenylalanine to phenyl pyruvic acid by L-amino acid deaminase. O_2 oxygen, NH_3 ammonia

In the aerobic reaction process no H_2O_2 is reportedly formed in contrast to other oxidases [44]. This raises the question of the classification of LAAD as a typical amine oxidase. In case LAAD is indeed no typical oxidase, it might point in the direction of a unique oxidase or the oxidase has some oxygenation activity [45]. Then the electron recycling system is to be determined. So far LAAD was just characterized in a whole-cell-environment. [43]

In order for conclusive characterization of structural-functional properties a soluble, isolated enzyme is necessary. No further details of successful soluble expression of the enzyme was reported when this work was done.

4.2 Aim of work

The aim of this work was the cloning, soluble expression, purification and further characterization of LAAD.

To realize this objective, various aims were required:

1. Creation and cloning of truncated LAAD variants
2. Expression of soluble, active LAAD in *E. coli*
3. Purification of obtained variants to apparent homogeneity for characterization
4. Basic characterization with respect to thermal stability, spectral properties and kinetics parameters
5. Determination of enzyme classification in regard to catalyzed reaction

4.3 Methods

4.3.1 Molecular biology procedures

Media preparation, calcium chloride heat shock transformation, PCR/DNA purification, plasmid isolation and gel electrophoresis were performed as described in section 3.3.1.

4.3.1.1 Cloning LAAD variants

The gene encoding for LAAD from *P. myxofaciens* was kindly provided by professor W. Kroutil from the University of Graz, Austria. The gene was cloned into the pET21a expression vector between the NdeI and Sall restriction sites [46].

The wildtype gene of LAAD is not expressed soluble in *E. coli* [43]. In order to get pure enzyme for further characterization a soluble LAAD enzyme was needed. Therefore the sequence of LAAD was analyzed for transmembrane helices using the TMHMM2.0 prediction service [47]. Based on these findings truncated variants of the LAAD gene were introduced into a template using a mutant strand synthesis PCR followed by *DpnI* digestion [31].

First the truncated version of LAAD (dLAAD) was constructed and then additional variants with corresponding primers. In dLAAD the first 29 aa of the LAAD sequence were deleted. dLAAD+1aa was based on dLAAD including the start codon ATG. The third variant dLAAD+1-6aa was based on dLAAD adding the first six original amino acids of the LAAD sequence in front. The primers are shown in Table 4-1.

Table 4-1 PCR primers for LAAD variants.

primer	sequence from 5'end to 3'end
LAAD forward	ATGAACATTTCAAGGAGAAAGCTAC
dLAAD forward	CGCCGTGATGGTAAATTTGTTG
(d)LAAD reverse	TTACTTCTTAAAACGATCCAAACTAAACG
dLAAD +1aa reverse	TACTTACTTCTTAAAACGATCCAAACTAAACG
dLAAD +1-6aa reverse	TACTTGTAAGTTCCTCTTTACTTCTTAAAACGATCCAAACTAAACG

The *PfuUltra* II Hotstart PCR Master Mix was used for the PCRs. The provided pET21a-LAAD construct was used as template in the PCRs for the LAAD variants. The PCR reaction set-ups and temperature profiles are listed in Table 4-2 and Table 4-3. The PCR products were purified and eluted in 40 μ L elution buffer.

Table 4-2 PCR reaction for LAAD variants.

component	volume [μ L]
2 x Mastermix <i>Pfu</i> Hotstart (buffer, enzyme, dNTPs, Mg^{2+})	10
10 μ M forward primer	0.5
10 μ M reverse primer	0.5
100 ng template	x
MilliQ	to end volume of 20

Table 4-3 Temperature profile of PCR reaction for LAAD variants.

PCR step	time [min]	temperature [°C]	
initial denaturation	2	95	
denaturation	0.5	95	} 20x
annealing	0.5	52	
extension	7.5	72	
final extension	10	72	
store	∞	8	

The purified PCR products were digested (2 h, 37°C) with *DpnI* and again purified. The DNA concentration was measured using the Nanodrop spectrophotometer and an agarose gel 0.8% was run to check availability of plasmid.

The generated blunt ended PCR products were phosphorylated (45 min, 37°C) by T4 polynucleotide kinase. Ligation was carried out (2 h and o/n, 37°C) with T4 Quick ligase. The phosphorylated, ligated plasmid was transformed in *E. coli* TOP 10 cells and plated (37°C, o/n) on LB-ampicillin plates (see section 3.3.1.4). Single colonies from the master plate were inoculated individually in 5 mL LB-ampicillin o/n at 37°C. On the next day the plasmids were isolated from *E. coli* TOP10 cells and sent to sequencing with the T7 forward primer. The mutated regions were sequenced.

4.3.1.2 Cloning LAAD in pET-SUMO vector

The dLAAD gene was cloned into the pET-SUMO vector for soluble expression according to the manual [28]. First a PCR of the truncated dLAAD gene was done as described in section 4.3.1.1. The designed primers (see Table 4-1) of dLAAD were used and pET21a-dLAAD was chosen as template. The PCR product was put on gel to check for availability and size.

With *Taq* polymerase adenine residues (A-overhangs) were added on the PCR product dLAAD for later Thymine/Adenine-cloning. In Table 4-4 the reaction set up is listed. 2046 ng of dLAAD was used and the reaction was incubated for 15 min at 72°C in a preheated heat block.

Table 4-4 Set-up to add A-overhangs to PCR products.

component	volume [μ L]
dLAAD	30
<i>Taq</i> polymerase	1
10x <i>Taq</i> buffer	4
10 mM dATP	2.5
MilliQ	2.5

The PCR product with A-overhangs (dLAAD+A) was purified and the concentration was measured with the Nanodrop spectrophotometer.

150 ng of dLAAD+A and 50 ng linear pET-SUMO vector were ligated (15 min, 25°C) with T4 Quick ligase. The ligation set-up can be seen in Table 4-5.

Table 4-5 Ligation set-up for pET-SUMO-dLAAD.

component	volume [μ L]
dLAAD+A	4.5
pET-SUMO	2
T4 Quick Ligase	10
2x T4 Quick Ligase buffer	2.5
MilliQ	3.5

The transformation was carried out with the Champion™ pET-SUMO Expression System kit. The used cells and SOC medium were taken from the kit. The whole ligation mix was incubated on ice for 20 min with one vial of One Shot Mach1 chemically competent cells. A heat shock was done for 30 s at 42°C. The ligation cell mixture was placed on ice for 1 min and 250 μ L SOC medium added. The cells were incubated at 37°C for 1 h and plated on LB-kanamycin plates (o/n, 37°C). Six single colonies were picked the next day and were inoculated individually in 5 mL LB-kanamycin o/n at 37°C. On the next day the plasmids were isolated and sent for sequencing using SUMO forward primer.

4.3.1.3 Factors affecting (d)LAAD expression

To improve expression of (d)LAAD different expression temperatures and shaking parameters and *E. coli* strains were tested.

4.3.1.3.1 Expression at different temperatures and shaking parameters

Protein expression was performed at three different temperatures and shaking parameters: 17°C at 180 rpm, 24°C at 135 rpm and 37°C at 200 rpm.

Initially pET21a-LAAD was transformed and expressed in *E. coli* BL21(DE3). For each temperature an o/n culture of *E. coli* BL21(DE3) from stock was diluted 1:100 in 5 mL LB-ampicillin and grown (37°C, 200 rpm) to an OD₆₀₀ of around 0.5.

Before induction the culture volume was spilt in half and marked as an uninduced (UI) and induced (I) sample. Cells were induced at room temperature with filter-sterilized IPTG at a final concentration of 1 mM and further cultivated at 17°C at 180 rpm, 24°C at 135 rpm and 37°C at 200 rpm. The uninduced samples were cultivated as the induced samples. As control, one culture per temperature was kept uninduced from the beginning.

In Table 4-6 an overview of the cultures expression conditions is shown.

Table 4-6 Expression sample overview of pET21a-LAAD *E. coli* BL21(DE3) cultures. x= sample, UI uninduced, I induced

sample time [h]	UI				I		
	0	2	4	o/n	2	4	o/n
temperature [°C]/ shaking [rpm]							
37 / 200	x	x	x		x	x	
24 / 135	x	x	x	x	x	x	x
17 / 180	x	x	x	x	x	x	x

After induction, 500 µL samples from all cultures were taken after 2 h, 4 h and o/n (21 h). From the 500 µL, 100 µL were taken for OD₆₀₀ measurements and the rest 400 µL samples were spun down (5 min, room temperature, 21 000 g) in 2 mL tubes.

The pellets were frozen for later use at -20°C. After sonication and separation of samples according to protocol A in section 4.3.1.5.2, the cell fractions were later analyzed by SDS-PAGE.

4.3.1.3.2 *Alternative E. coli strains*

Additional *E. coli* strains were tested as expression hosts for dLAAD+1aa. pET21a-dLAAD+1aa and empty pET21a were used as vectors. The following strains were investigated: *E. coli* BL21(DE3), *E. coli* C41(DE3) and *E. coli* C43(DE3). Transformation of competent *E. coli* cells and both vectors were carried out as described in 3.3.1.4.

The *E. coli* BL21(DE3) cells with no plasmid were grown in LB without antibiotic as negative expression control.

Plasmid containing strains were cultivated as described in section 4.3.1.3.1 and expression of dLAAD+1aa was induced at a final IPTG concentration of 1 mM when OD₆₀₀ reached a value of 0.5. Protein expression was conducted at 180 rpm either o/n at 16°C or for 48 h at 17°C. Cell density was measured from resultant cell suspensions and cell pellets were prepared in 2 mL samples by centrifugation (5 min, room temperature, 21 000 g) and stored at -20°C. After sonication and separation of samples according to protocol A in section 4.3.1.5.2, the cell fractions were later analyzed by SDS-PAGE. The frozen pellets were used as well for activity assay experiments.

4.3.1.4 *Preparation of alditol oxidase*

For the redox dye activity tests the known soluble expressed alditol oxidase (AldO) was chosen as an enzyme control. Therefore a pBAD-MBP-AldO construct [48] was transformed into *E. coli* Top 10 according to section 3.3.1.4. The pBAD vector carried an ampicillin resistance and was induced with L-arabinose (0.02% (w/v) final concentration). The construct was provided by professor M. Fraaije from the University of Groningen, Netherlands. The enzyme was expressed as described above in section 4.3.1.3.2. The *E. coli* BL21(DE3) cells containing AldO were sonicated according to section 3.3.1.13 and spun down (5 min, room temperature, 21 000 g). Portions of the cell free extract with AldO were used for the activity tests.

4.3.1.5 **Purification of (d)LAAD**

Three purification protocols were worked out for later experiments. All protocols involved sonication and/or multiple centrifugation steps and the use of a detergent. Purification protocol A and B were established to determine the precise location of truncated dLAAD+1-6aa in the cell. Purification protocol C was developed for samples used in section 4.3.2.3.2.

Expression of *E. coli* BL21(DE3) cells were carried out as described in section 4.3.1.5.1.

4.3.1.5.1 *Expression for purification protocols*

For protocol A and B dLAAD+1-6aa and for protocol C LAAD were expressed in *E. coli* BL21(DE3). Control experiments were performed with *E. coli* cells harbouring the empty pET21a vector.

For all cell cultures an o/n culture of *E. coli* BL21(DE3) with the respective plasmid was diluted 1:100 in TB-ampicillin and grown (37°C, 200 rpm) to an OD₆₀₀ of around 0.5. Induction was initiated with final 1mM IPTG. From the time of induction all cells (uninduced and induced samples) were cultivated for 72 h, at 17°C and at 180 rpm. OD₆₀₀ values were measured from the resultant cell suspension and cell pellets prepared by centrifugation (5 min, room temperature, 21 000 g) and stored at -20°C.

4.3.1.5.2 *Purification protocol A*

The expressed and unexpressed dLAAD+1-6aa cell pellets and cell pellets containing pET21a were thawed and resuspended in 500 µL 50 mM Tris/HCl pH 7.5. The buffer contained Deoxyribonuclease I (DNase I) (0.1 mg/mL final concentration) and magnesium sulfate (MgSO₄) (5 mM final concentration) to reduce viscosity for SDS-PAGE. The cells were sonicated.

The purification protocol A is illustrated in Figure 4-2.

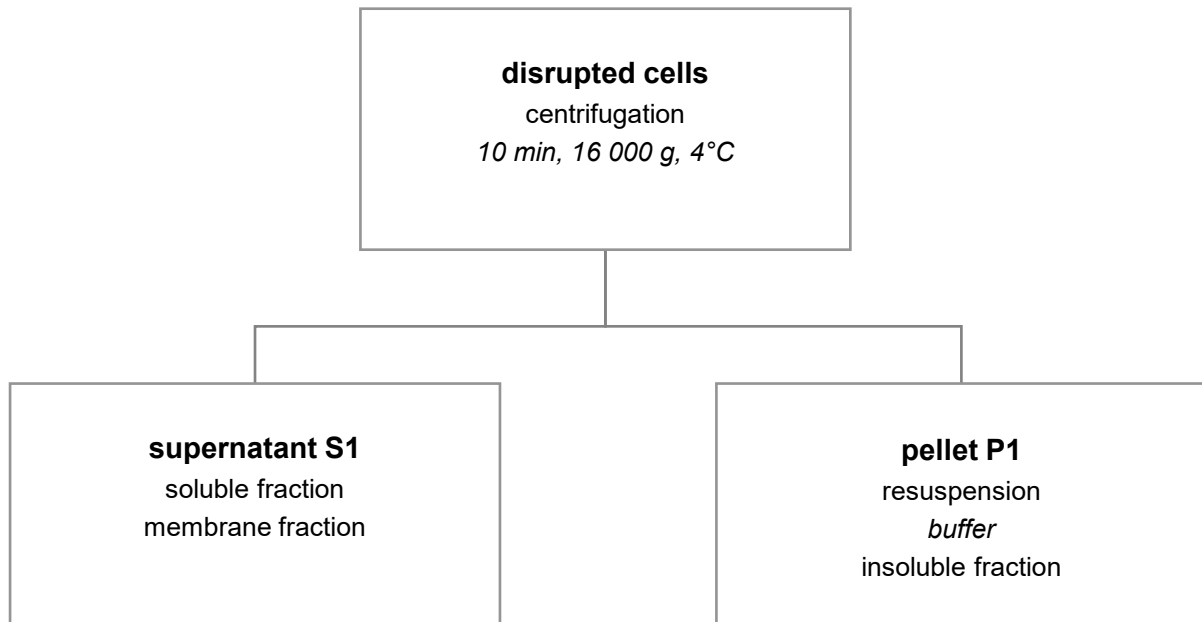


Figure 4-2 Purification protocol A. *buffer 50 mM Tris/HCl pH 7.5 150 mM NaCl*

Samples WC (whole cell), S1 and P1 were analyzed by SDS-PAGE.

4.3.1.5.3 Purification protocol B

The expressed and unexpressed dLAAD+1-6aa cell pellets and cell pellets containing pET21a were thawed and resuspended in 500 μ L 50mM Tris/HCl pH 7.5 for sonication. Before sonication, a 50 μ L sample (WC) was taken for SDS-PAGE analysis. The remaining 450 μ L of cells were sonicated.

A flow sheet displaying the purification centrifugation steps and detergent treatments is shown in Figure 4-3.

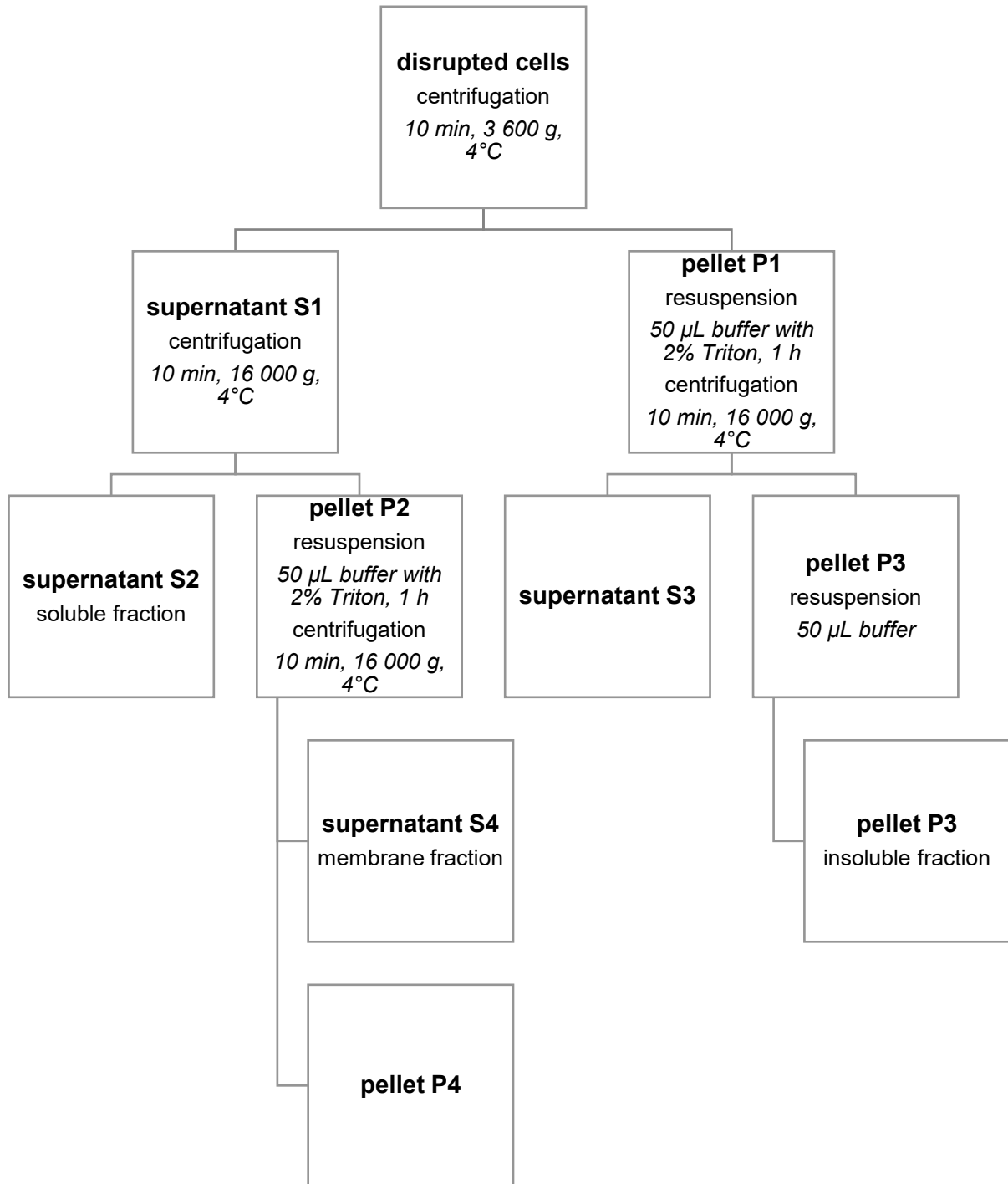


Figure 4-3 Purification protocol B. *buffer 50 mM Tris/HCl pH 7.5 150 mM NaCl*

Samples WC, S2, S3, S4, P3, P4 were analyzed by SDS-PAGE. All samples were mixed with 2x SDS Loading dye, heated (5 min, 80°C) and spun down (15 min, 4000 rpm). The prepared samples were put onto 12% SDS gels.

4.3.1.5.4 Purification protocol C

Protocol C was used to separate the soluble, membrane and insoluble fraction of expressed LAAD cells and cells containing the empty vector. The cells were thawed and resuspended in 500 μ L 50 mM Tris/HCl, pH 7.5 containing DNase I (0.1 mg/mL final concentration) and MgSO₄ (5 mM final concentration). The cells were broken up by sonification and cell fractions were separated as depicted in Figure 4-4.

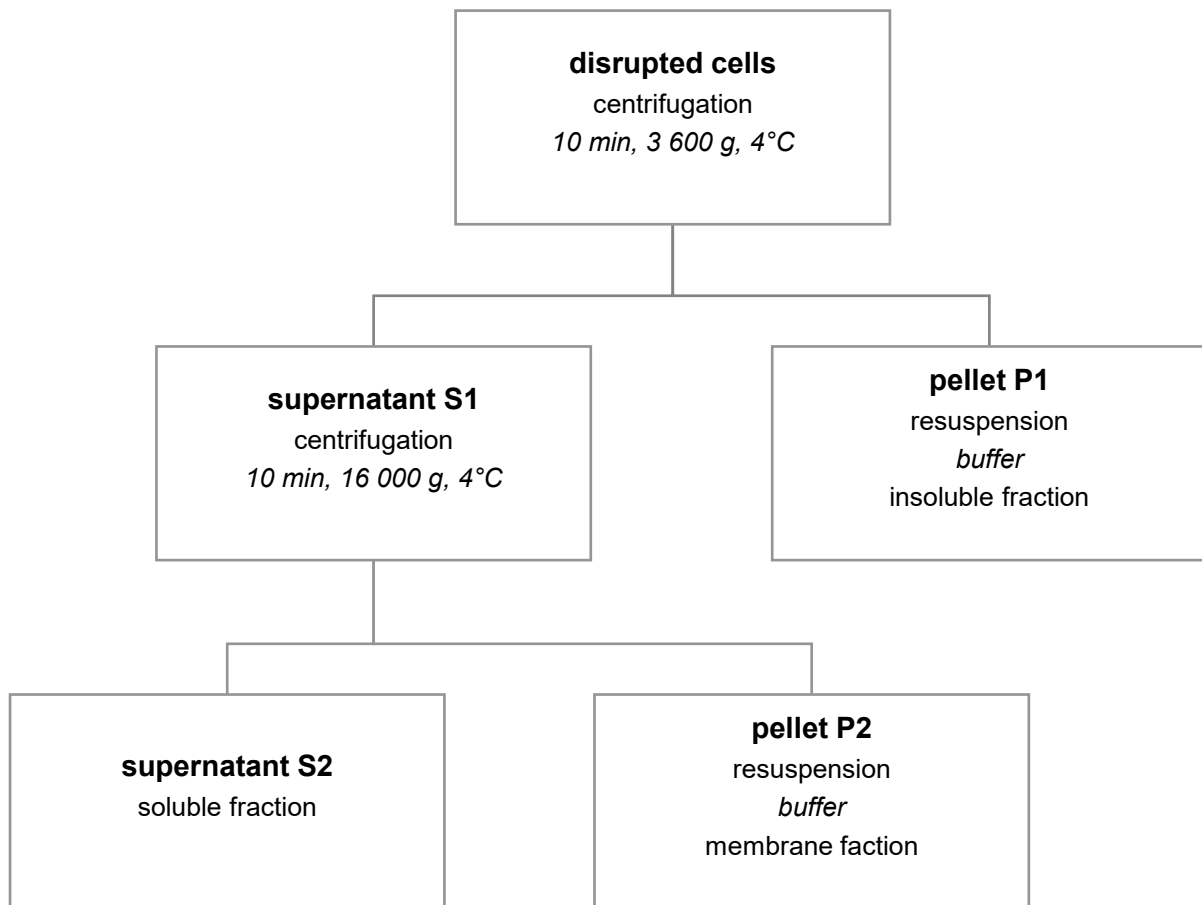


Figure 4-4 Purification protocol C. *buffer 50 mM Tris/HCl pH 7.5 150 mM NaCl*

The pellets P1 and P2 of the different cells were resuspended and diluted in buffer according to the base OD₆₀₀ measurements (see section 4.3.1.5.1). The prepared samples S1, S2, P1 and P2 were used for experiments in section 4.3.2.3.

4.3.2 Analytics

4.3.2.1 Activity assays

The determination of enzyme classification in regard to catalyzed reaction was investigated in whole-cell experiments. Two activity tests were performed to determine whether (d)LAAD catalyzed oxidation or oxidoreductase type reactions.

4.3.2.2 Oxidase assay

The oxidase assay was carried out by following a coupled reaction to be seen in Figure 4-5. Through the simultaneous horseradish peroxidase (HRP) catalyzed reaction between 4-Aminoantipyrine (AAP), 3,5-Dichloro-2-hydroxybenzenesulfonic acid (DCHBS) and hydrogen peroxide (H_2O_2), which was produced in the oxidase catalyzed reaction, a pink or purple product was formed.

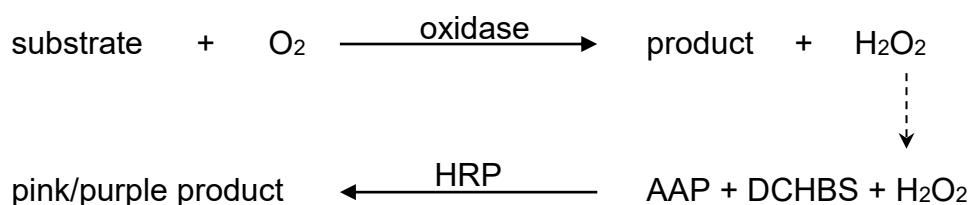


Figure 4-5 Oxidase assay underlying reaction pathway AAP 4-Aminoantipyrine, DCHBS 3,5-Dichloro-2-hydroxybenzenesulfonic acid, HRP horseradish peroxidase

The accumulation of this product was determined by measuring its absorbance at 515 nm with a spectrophotometer. The molar extinction coefficient ϵ_{515} of the product was $26 \text{ mM}^{-1}\text{cm}^{-1}$. Provided that the HRP catalyzed reaction immediately used any hydrogen peroxide present to form the colored product, the build-up of product was a sign of the oxidation reaction catalyzed by any oxidase. [48]

For the oxidase test *E. coli* BL21(DE3) expressing LAAD and dLAAD+1aa, *E. coli* C41(DE3) expressing dLAAD+1aa and *E. coli* BL21(DE3) cells were tested. The prepared cell pellets were resuspended according to a base OD_{600} of 1.15 and diluted in 50 mM Tris/HCl buffer pH 7.5 containing 150 mM NaCl and DNase I (0.1 mg/mL

final concentration) and MgSO₄ (5 mM final concentration). The sonicated samples were not spun down but used as whole cell fractions.

Cell-free extract containing AldO was used as positive control. Reference measurements without HRP and without substrate were also carried out.

L-phenylalanine was the chosen substrate for all (d)LAAD samples. For AldO xylitol was used as substrate. AldO converted xylitol to D-xylose as to be seen in Figure 4-6 [48].



Figure 4-6 Conversion of xylitol to D-xylose by AldO. *AldO alditol oxidase*

The oxidase reaction was carried out at room temperature with 0.1 mM AAP, 1.0 mM DCHBS, 4 U HRP, 1 mM L-phe or 0.5 mM xylitol as substrate and filled up with 50 mM KPi buffer pH 7.5 to a final volume of 200 μ L. All mentioned concentrations were final concentrations. After adding the 30 μ L whole cell fractions (diluted with buffer to a base OD₆₀₀ of 1.15) the reaction was started. The 200 μ L sample was divided and the reaction was carried out with 100 μ L for each time point. Before measuring absorption at 515 nm with the Synergy Mx spectrophotometer, the samples were spun down after 2.5 and 24 h.

4.3.2.3 Oxidoreductase assay

To identify any oxidoreductase activity of LAAD a qualitative colorimetric assay with redox indicators was applied. The redox dyes methylene blue (MB), methylene green (MG) and 2,6-dichlorophenol-indophenol (DCPIP) were chosen. If the redox dye was reduced upon a redox reaction, an absorption change occurred and a visible color change could be monitored. [49]

In the FAD catalytic cycle, the regeneration of oxidized FAD was possible using substitute electron acceptors. [44] The redox systems of the redox dyes could serve as alternative electron acceptors.

Upon reaction MB and MG were oxidized by a two electron and one proton transfer, respectively as seen in Figure 4-7, resulting in a blue or green to colorless visible color

change. MB and MG color changes can be monitored by measuring absorption at 668 nm and 655 nm, respectively. [49] [50]

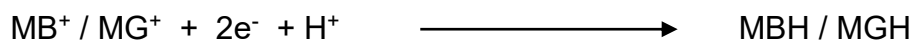


Figure 4-7 Redox reaction of methylene blue und methylene green.
MB methylene blue, MG methylene green

DCPIP undergoes a two electron and two proton transfer process as can be seen in Figure 4-8. Oxidized, blue DCPIP turned colorless as DCPIP was reduced. The decolorization were followed at 520 nm. [49] [51]



Figure 4-8 Redox reaction of DCPIP *DCPIP 2,6-dichlorophenol-indophenol*

4.3.2.3.1 Redox dye testing

To test which redox indicator was suitable for LAAD all three redox dyes were tested. For the redox dye test the same cells as in section 4.3.2.2 were used. L-phe was taken as substrate for all (d)LAAD samples.

All mentioned concentrations were final concentrations. The reaction was carried out with 1 mM L-phe or 0.5 mM xylitol as substrate, 0.075 mM MB or 0.1 mM MG or 0.45 mM DCPIP as redox dye and filled up with 50 mM Tris/HCl buffer pH 7.5 to a final volume of 200 μL . After adding the 30 μL sonicated whole cell fractions (diluted with buffer to a base OD_{600} of 1.15) the reaction was started. The 200 μL sample was divided and the reaction was carried out with 100 μL for each time point. Before measuring absorption, the samples were spun down after 2.5 and 24 h.

4.3.2.3.2 DCPIP oxidoreductase assay

To measure the level of oxidoreductase activity in different fractions of *E. coli* BL21(DE3) cells expressing LAAD or carrying pET21a a DCPIP oxidoreductase assay was made. The S1, S2, P1 and P2 cell fractions of these cells (see section 4.3.1.5.4) were used.

The test was set up with 1 mM L-phe as substrate, 0.9 mM DCPIP as redox dye and filled up with 50 mM Tris/HCl buffer pH 7.5 to a final volume of 200 μ L. All mentioned concentrations were final concentrations. After adding 20 μ L of protein samples from S1, S2, P1 and P2 the reaction was started. The absorption was measured at 520 nm for 30 min. Reference reactions without protein sample, without substrate and just redox dye were made. The protein concentrations of the samples were determined as described in section 4.3.2.4.

The reaction in the DCPIP assay was followed at 520 nm and a molar extinction coefficient ϵ_{520} of 6.6 $\text{mM}^{-1}\text{cm}^{-1}$ [49] for a reaction pH above 6.5 was used.

The relative absorption change was determined by following the absorption decrease [mOD] over time [min] for 30 min. The relative absorption change was calculated by Equation 4. ΔA_λ stands for the relative absorption change at 520 nm [mODmin^{-1}], A_t for the absorption measured at the time point t and A_0 for the initial absorption.

$$\Delta A_\lambda = \frac{A_t}{A_0} * 100 \quad \text{Equation 4}$$

Using Microsoft Excel, the resulting mOD/min measurements were converted to OD/min. Using the law of Lambert Beer in Equation 1 the total enzyme activity of the cell solution could be calculated.

In this use of Equation 1, A_λ stands for relative absorption change ΔA_λ at 520 nm [ODmin^{-1}], ϵ_λ for molar extinction coefficient of the DCPIP with ϵ_{520} of 6.6 $\text{mM}^{-1}\text{cm}^{-1}$, c for total enzyme activity of the cell solution [mMmin^{-1}] and d for the changing pathlength [cm]. The distance of the light path was measured by the spectrometer at 0.3 to 0.5 cm for each sample.

The given enzyme activity measurements were corrected for the background reference measurements without substrate. An average was calculated out of the double measurements of each sample.

With the used final protein concentrations [mg mL^{-1}] determined by the Bradford assay the average specific enzyme activities [$\mu\text{Mmin}^{-1}\text{mg}^{-1}$] of all samples were calculated.

4.3.2.4 Bradford assay

Determination of the protein quantity was measured by the Bradford assay. This was accomplished by measuring the absorbance from Coomassie brilliant blue G-250 (Bradford reagent) at 595 nm. The increase of absorbance was directly connected to the amount of bound dye to the existing protein concentration. [52]

A standard curve was generated with known bovine serum albumin (BSA) concentrations from 0.0625 mg/mL to 1 mg/mL.

5 μL of protein samples from S1, S2, P1 and P2 (see section 4.3.1.5.4) were mixed with 200 μL of ready-to-use Bradford reagent, incubated for 10 min at room temperature and read at 595 nm. As buffer for the standard curve and for diluting samples S1 and S2 1:5, 50 mM Tris/HCl pH 7.5 was used. The standard curve and the protein samples preparation were made in parallel and in duplicates.

The BSA standard curve was then used to determine the unknown protein concentrations of all samples. The measured final concentrations [mg mL^{-1}] of all samples were then adjusted according to the sample use of 20 μL and used for the specific activity calculations in section 4.3.2.3.2.

4.4 Results

4.4.1 Transmembrane helix prediction and LAAD variants design

For characterization of LAAD a soluble enzyme was required. The sequence of LAAD was analyzed for transmembrane helices using the TMHMM2.0 prediction service. The program indicated a transmembrane helix being formed from the 7th to 29th aa of the sequence. According to the prediction three truncated LAAD variants were created: dLAAD, dLAAD+1aa, dLAAD+1-6aa.

In dLAAD the first 29 aa of LAAD were deleted and so the sequence started with the 30th aa. The variant dLAAD+1aa consisted of the introduced start codon ATG followed by dLAAD. dLAAD+1-6aa was designed consisting out of the first original six amino acids of LAAD followed by dLAAD. In Figure 4-9 a schematic overview of all variants can be seen.

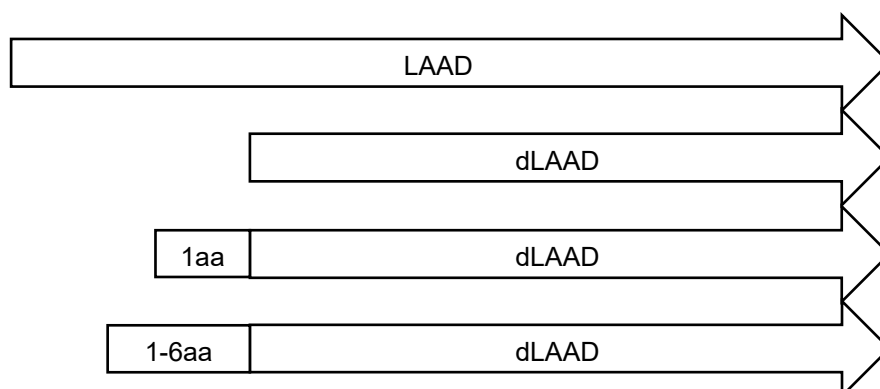


Figure 4-9 Schematic overview of all LAAD variants. *aa amino acid*

4.4.2 Cloning LAAD variants

Three variants of the gene encoding LAAD were amplified and mutated with specific primers from the pET-21a-LAAD template. Resulting in three new LAAD variant constructs: pET21a-dLAAD, pET21a-dLAAD+1aa and pET21a-dLAAD+1-7aa.

pET21a-dLAAD and pET21a-dLAAD+1aa were successfully created and checked by sequencing. Sequencing of supposed pET21a-dLAAD+1-6aa revealed that an

additional seventh amino acid was introduced through the designed primers. The new construct was named pET21a-dLAAD+1-7aa and used for further experiments. All three constructs were transformed and expressed in *E. coli*. In Table 4-7 an overview of the three LAAD variants is listed.

Table 4-7 Overview of LAAD and its three variants.

variant	nucleotide sequence	amino acid sequence
	[bp]	[aa]
LAAD	1425	474
dLAAD	1338	445
dLAAD+1aa	1341	446
dLAAD+1-7aa	1359	452

In Figure 4-10 and Figure 4-11 the beginnings of sequence alignments are shown and common features highlighted.



Figure 4-10 5'-3' beginning of nucleotide sequence alignment of all LAAD variants. Nucleotide sequences of 1-29 aa are underlined black, 1aa light grey, 1-7aa dark grey. * indicates start of aligning sequence, the box highlights the same starting sequence

```

LAAD           MNISRRK|LLLGVGAAGVLAGGAATLVPMVRRDGKFVESKSRALFVESTEGALPSES DVVI
dLAAD         -----RRDGKFVESKSRALFVESTEGALPSES DVVI
dLAAD+1aa     -----MRRDGKFVESKSRALFVESTEGALPSES DVVI
dLAAD+1-7aa   -----MNISRRK|RRDGKFVESKSRALFVESTEGALPSES DVVI
                *****
    
```

Figure 4-11 5'-3' beginning of amino acid sequence alignment of all LAAD variants. Amino acid sequences of 1-29 aa are underlined black, 1aa light grey, 1-7aa dark grey. * indicates start of aligning sequence, the box highlights the same starting sequence

4.4.3 Cloning LAAD in pET-SUMO

The gene encoding dLAAD was amplified from the pET-21a-LAAD template, ligated into the pET-SUMO plasmid and transformed into *E. coli*. Four colonies were grown and analyzed. The isolated pET-SUMO-dLAAD construct was checked by electrophoresis and sequencing. It was revealed that no plasmid was present on the control gel. The sequencings results were negative and confirmed the conclusion. The pET-SUMO-cloning attempt was not continued in this work.

4.4.4 Factors affecting (d)LAAD expression

Different expression temperatures and shaking parameters as well as *E. coli* strains were tested to enhance expression of LAAD and dLAAD+1aa.

4.4.4.1 Expression at different temperatures and shaking parameters

Protein expression of LAAD in *E. coli* BL21(DE3) at 17°C at 180 rpm, 24°C at 135 rpm and 37°C at 200 rpm were monitored by taking induced and uninduced samples at 2 h, 4 h and o/n (21 h) after induction. The SDS-PAGE gels of all samples showed no significant increase of expressed protein depending on temperature and shaking parameters.

4.4.4.2 Alternative *E. coli* strains

E. coli C41(DE3) and *E. coli* C43(DE3) were tried as alternative expression hosts for dLAAD+1aa. Expression was done at 16 or 17°C for at least 48 hours after induction to promote better protein folding. The analysis of the SDS-PAGE gels of the truncated protein showed no enhanced protein expression compared to *E. coli* BL21(DE3) cells. As example, the typical found background pattern of *E. coli* cells can be seen in Figure 4-12.

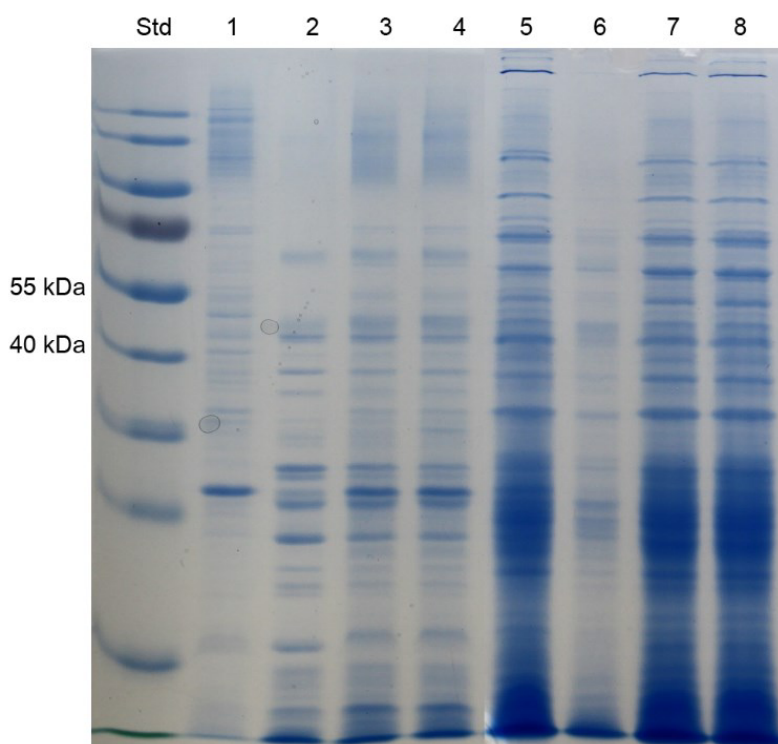


Figure 4-12 12% SDS-PAGE gel of different cell fractions following the protein purification protocol A of induced and sonicated *E. coli* BL21(DE3), C43(DE3), and C41(DE3) containing pET-21a-dLAAD+1aa or pET21a vector. dLAAD+1aa at 51 kDa. Supernatant samples contain the soluble and membrane fraction and pellet samples the insoluble fraction. *S* supernatant, *P* pellet

Std PageRuler™ Prestained Protein Ladder

Slot 1 – 4 pellet samples **Slot 1** pET21a BL21(DE3), **Slot 2** dLAAD+1aa BL21(DE3), **Slot 3** dLAAD+1aa C43(DE3), **Slot 4** dLAAD+1aa C41(DE3)

Slot 5 – 8 supernatant samples **Slot 5** pET21a BL21(DE3), **Slot 6** dLAAD+1aa BL21(DE3), **Slot 7** dLAAD+1aa C43(DE3), **Slot 8** dLAAD+1aa C41(DE3)

4.4.5 Localization of dLAAD in the cell

In order to determine the location in the cell of expressed dLAAD+1-7aa and the potential of inclusion body formation protein purification was done.

Sonicated *E. coli* BL21(DE3) cells containing pET21a-dLAAD+1-7aa and pET21a were separated following purification protocol A and B and analyzed on 12% SDS-PAGE gels.

First a general purification protocol A was followed. The disrupted cells samples got separated by one fast centrifugation step. The supernatant S1 samples contained the soluble and membrane fraction and pellet P1 samples the insoluble fraction. The results are given in Figure 4-13. Slot 1 shows a slight overexpressed band at 51 kDa in the less concentrated whole cell fraction. In slot 2 a clear formation of inclusion bodies of overexpressed dLAAD+1-7aa in sample P1 can be seen at around 51 kDa. The uninduced dLAAD+1-7aa and empty vector samples show no higher expression of dLAAD+1-7aa.

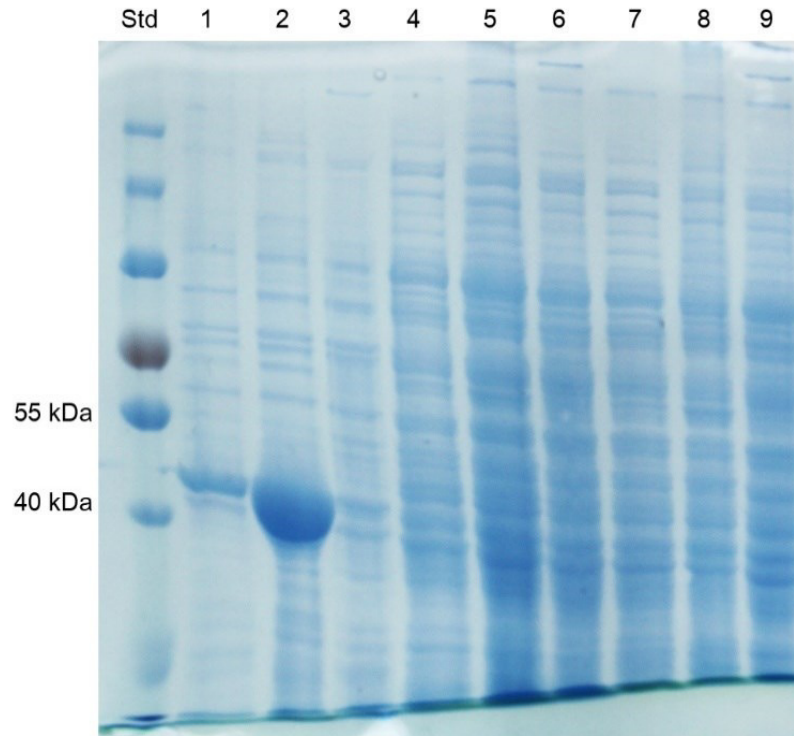


Figure 4-13 12% SDS-PAGE gel of different cell fractions following the protein purification protocol A of sonicated *E. coli* BL21(DE3) containing pET-21a-dLAAD+1-7aa or pET21a vector. dLAAD+1-7aa at 51 kDa. S1 samples contain the soluble and membrane fraction and P1 samples the insoluble fraction. *S* supernatant, *P* pellet

Std PageRuler™ Prestained Protein Ladder

Slot 1 – 3 dLAAD1-7aa cell fraction samples **Slot 1** whole cell, **Slot 2** P1, **Slot 3** S1

Slot 4 – 6 uninduced dLAAD1-7aa cell fraction samples **Slot 4** whole cell, **Slot 5** P1, **Slot 6** S1

Slot 7 – 9 pET21a cell fraction samples **Slot 7** whole cell, **Slot 8** P1, **Slot 9** S1

Next a purification protocol B was established to get a more detailed insight of the precise location of dLAAD+1-7aa in the cell. Therefore, the disrupted cells were further separated by fast and slow centrifugation steps combined with detergent treatments. The supernatant S2 samples contained the soluble membrane fraction, the supernatant S4 samples the membrane fraction and pellet P3 samples the insoluble fraction. Sample P3 and all whole cell samples of cells expressing dLAAD+1-7aa were too viscous to put on the gel.

In Figure 4-14, the comparison of different cell fractions with induced and uninduced expression of dLAAD+1-7aa can be seen. Slot 14 shows a strong formation dLAAD+1-7aa inclusion bodies in the insoluble fraction P3 at around 51 kDa. No overexpressed dLAAD+1-7aa is to be seen in the membrane fraction in slot 13 in comparison with the uninduced sample in slot 10.

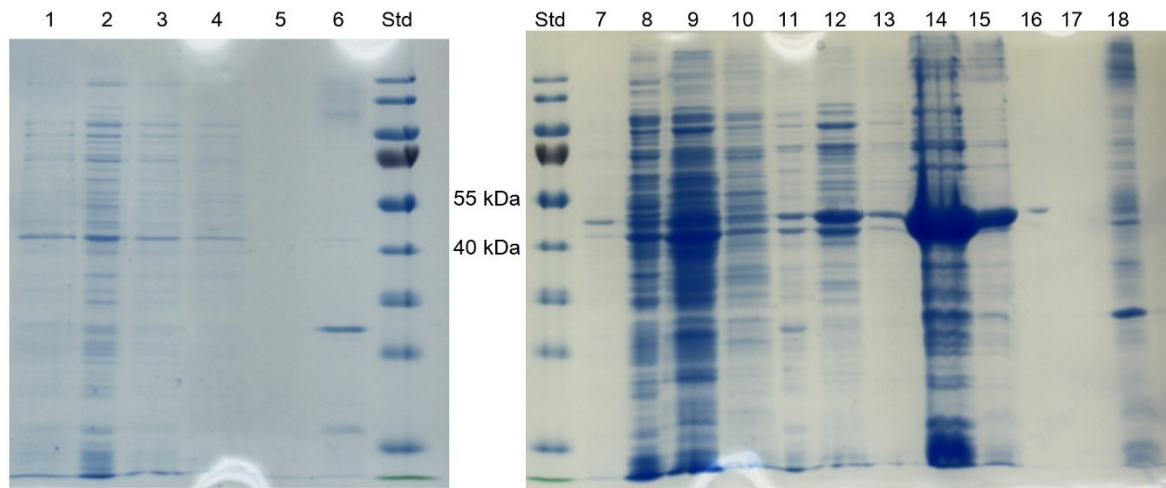


Figure 4-14 12% SDS-PAGE gel of different cell fractions following the protein purification protocol B sonicated *E. coli* BL21(DE3) containing pET-21a-dLAAD+1-7aa or pET21a vector. dLAAD+1-7aa at 51 kDa. S2 samples contain the soluble fraction, S4 samples the membrane fraction and P3 samples the insoluble fraction. *S supernatant, P pellet*

Std PageRuler™ Prestained Protein Ladder

Slot 1 – 6 pET21a cell fraction samples **Slot 1** whole cell, **Slot 2** S2, **Slot 3** S3, **Slot 4** S4, **Slot 5** P3, **Slot 6** P4

Slot 7, 16, 17 empty slots

Slot 8 – 10, 18 uninduced dLAAD1-7aa cell fraction samples **Slot 8** S2, **Slot 9** S3, **Slot 10** S4, **Slot 18** P4

Slot 11 – 15 expressed dLAAD1-7aa cell fraction samples **Slot 11** S2, **Slot 12** S3, **Slot 13** S4, **Slot 14** P3, **Slot 15** P4

4.4.6 Activity assays

A possible oxidase or oxidoreductase activity of (d)LAAD was tested with activity assays in whole-cell experiments.

4.4.6.1 Oxidase assay

To gain insight in any oxidase activity a coupled reaction oxidase assay was applied. In this assay any produced hydrogen peroxide (by an oxidase) was used by HRP to catalyze the formation of a colored product. Any colorization was followed by measuring its absorbance at 515 nm with a spectrometer after 2.5 and 24 h.

The sonicated samples were not spun down but used as whole cell fractions. L-phe was taken as substrate for all LAAD and dLAAD+1aa samples. Cell-free extract containing AldO was chosen as positive control. Reference measurements without HRP and without substrate were made.

The results of the oxidase activity assay are represented below in Figure 4-15. All whole cell samples showed the same level of oxidase activity. In comparison with the alditol oxidase sample, no oxidase activity due to LAAD/dLAAD+1aa could be seen in the expressed *E. coli* samples. They show a comparable level of oxidase activity as the negative control, *E. coli* BL21(DE3) cells.

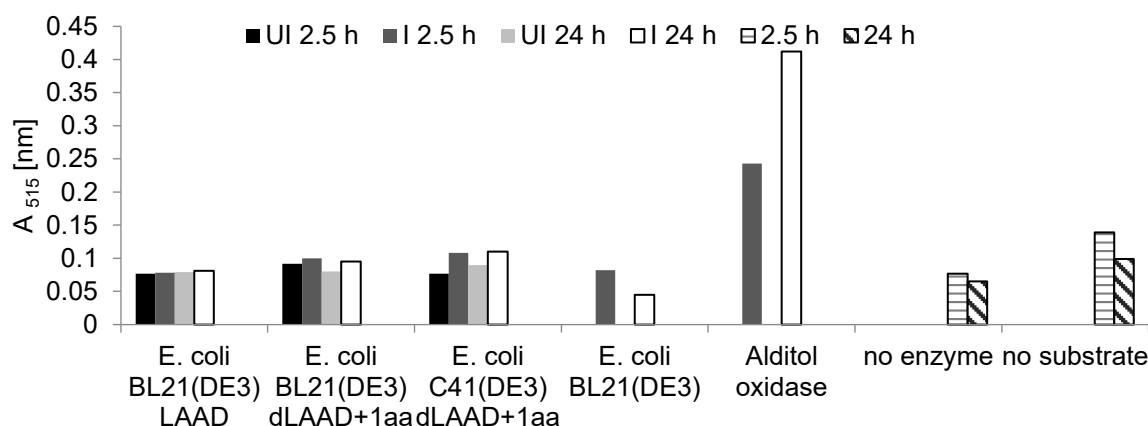


Figure 4-15 Oxidase assay with different sonicated *E. coli* cells expressing LAAD or dLAAD+1aa. 50 mM potassium phosphate buffer pH 7.5 was used. Reactions were stopped and the absorption measured at 515 nm after 2.5 and 24 h. Alditol oxidase was used as positive control. *UI uninduced, I induced*

4.4.6.2 Oxidoreductase assay

A qualitative colorimetric assay with redox indicators was used to prove any oxidoreductase activity of (d)LAAD.

4.4.6.2.1 Redox dye testing

The tested redox dyes were methylene blue, methylene green and 2,6-dichlorophenol-indophenol.

After adding the sonicated whole cell fractions the reaction was started, stopped and spun down after 2.5 and 24 h before measuring absorption. L-phe was taken as substrate for all LAAD and dLAAD+1aa samples.

All reactions with expressed LAAD or dLAAD+1aa with methylene blue or methylene green resulted in no clear visible color changes.

In Figure 4-16, the results of the DCPIP redox dye test assay are listed. A visible color change in all samples could be measured and confirmed DCPIP as a general suitable redox dye.

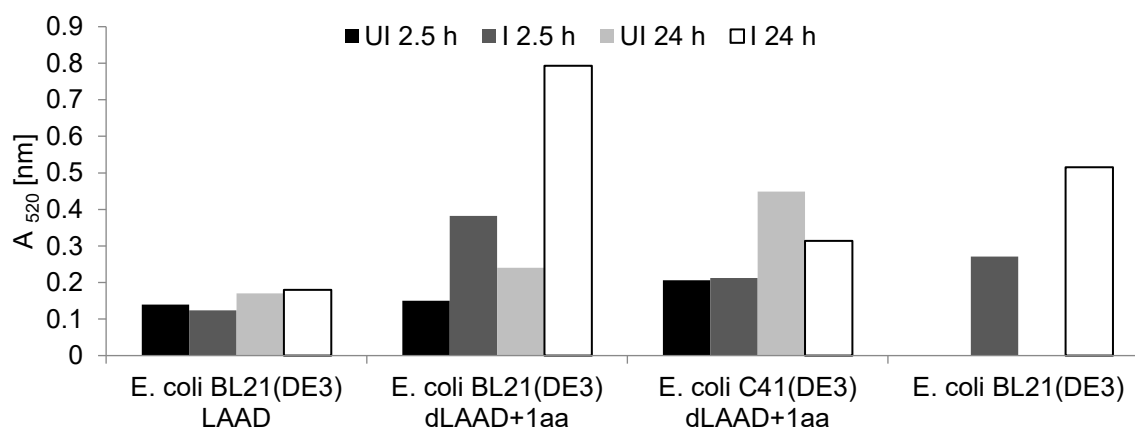


Figure 4-16 DCPIP redox dye test assay with different sonicated *E. coli* cells expressing LAAD or dLAAD+1aa. 50 mM Tris/HCl buffer pH 7.5 was used. Reactions were stopped and the absorption measured at 520 nm after 2.5 and 24 h. *UI* uninduced, *I* induced

4.4.6.2.2 DCPIP oxidoreductase assay

A DCPIP oxidoreductase assay was done to determine the level of oxidoreductase activity in different fractions of the cell. pET21a-LAAD and pET21a *E. coli* BL21(DE3) cells were sonicated and separated following protocol C. L-phe was taken as substrate for all LAAD samples. The pellet P1 samples contained the insoluble fraction, the supernatant S2 samples the soluble fraction and pellet P2 samples the membrane fraction.

With adding the cells fractions the reaction was started and the absorption was measured at 520 nm for 30 min. Reference reactions without cell fraction sample, without substrate and just redox dye were made.

The protein concentrations of the samples were determined using the Bradford assay and are listed in Table 4-8. In comparison to the pellet samples, the higher protein concentrations could be found in the supernatant samples. The factor of concentration difference was 1:10 and higher in the cells containing pET21a. The expression of LAAD shifted this ratio closer to 1:2 or 1:3.

Table 4-8 Protein concentrations of cell fraction samples of *E. coli* BL21(DE3) cells expressing LAAD or containing vector pET21a. S supernatant, P pellet

cell fractions	protein concentration [mgmL ⁻¹]	
	<i>E. coli</i> BL21(DE3) cells expressing LAAD	<i>E. coli</i> BL21(DE3) cells containing pET21a
S1	0.62	1.23
P1	0.33	0.18
S2	0.82	1.11
P2	0.24	0.38

With the used final protein concentrations [mgmL⁻¹] determined by the Bradford assay the average specific enzyme activities [$\mu\text{molmin}^{-1}\text{mg}^{-1}$] of all samples were calculated. Surprisingly, there was a very clear difference in the overall average specific enzyme activity between the cells expressing LAAD or containing the empty vector.

The highest average specific enzyme activity with $969 \mu\text{molmin}^{-1}\text{mg}^{-1}$ was found in the membrane fraction of the cells expressing LAAD, followed by the insoluble fraction

with $785 \mu\text{molmin}^{-1}\text{mg}^{-1}$. The supernatant fractions showed a similar high activity of around $360 \mu\text{molmin}^{-1}\text{mg}^{-1}$.

The cells containing pET21a displayed almost no specific enzyme activity.

Table 4-9 Average specific enzyme activity of cell fraction samples *E. coli* BL21(DE3) cells expressing LAAD or containing vector pET21a.

S supernatant, P pellet

cell fractions	average specific enzyme activity [$\mu\text{molmin}^{-1}\text{mg}^{-1}$]	
	<i>E. coli</i> BL21(DE3) cells expressing LAAD	<i>E. coli</i> BL21(DE3) cells containing pET21a
S1	355	18
	± 7	± 5
P1	785	0 ^{a)}
	± 130	
S2	368	0 ^{a)}
	± 55	
P2	969	0 ^{a)}
	± 3	

a) negative values corrected to 0

4.5 Discussion

4.5.1 Cloning LAAD variants

To shed more light on the enzyme classification of LAAD as an amine oxidase the production of soluble enzyme was the goal.

The pET21a vector served as a good basis for basic cloning and expression experiments. It provides inducible expression of N-terminally T7-tagged proteins. Furthermore, it was used in a protocol for expression of LAAD provided with the gifted pET-21a-LAAD [46].

Based on predicted transmembrane helix formed between the 7th and 29th aa three truncated versions of LAAD were designed. dLAAD was missing the supposed helix and served as basis for the creation of the two other variants. dLAAD+1aa had a start codon and dLAAD+1-7aa the first seven original LAAD amino acids added in front. This was done in case more than the start codon would be necessary for initiating successfully translation and folding. dLAAD and dLAAD+1aa variants were cloned. Due to a mistake made in the primer design for the supposed dLAAD+1-6aa variant, an additional amino acid was introduced and dLAAD+1-7aa was created.

The attempt of cloning LAAD in the pET-SUMO vector was not successful due to not further investigated cloning issues. So, this approach was not continued in this work.

4.5.2 Factors affecting (d)LAAD expression

Recombinant protein expression in *E. coli* can be a complicated process and depends on a lot of factors such as host strain, used plasmid, protein inactivation or expression conditions. [53] In this work different expression conditions and *E. coli* strains were tested to enhance expression of LAAD and dLAAD+1aa.

The three chosen combined factors of temperature and aeration (17°C at 180 rpm, 24°C at 135 rpm and 37°C at 200 rpm) were not leading to a difference in protein expression.

LAAD is a known membrane protein [43]. The overexpression of membrane protein is more complex and challenging than of cellular proteins [54]. In addition it was implied

in literature that high concentration of overexpressed LAAD might be toxic for the cell [55]. To take this hypothesis into account, *E. coli* strains C41(DE3) and C43(DE3) were chosen because of their effectiveness in expressing toxic and membrane proteins [56]. Unfortunately, the use of alternative *E. coli* hosts was not affecting the level of expressed LAAD.

In both experiments the SDS-PAGE gels just showed the typical *E. coli* background protein pattern under all conditions.

4.5.3 Localization of dLAAD in the cell

In order to see if the truncation of LAAD of any variant led to soluble expression, their location in the cell was investigated. Purification protocols were established to reach different grades of separation of cell fractions.

Regrettably, no enrichment of membrane protein containing any dLAAD variants could be seen. A strong formation of inclusion bodies in the insoluble fraction was found instead.

Some time after the practical work of this project was finished, LAAD was expressed successfully [57]. In that study the identified transmembrane helix was composed of the first 28 amino acids, the same (with one aa difference) compared to that in this thesis. Variants with different deletions of N-terminal segments (a variant starting at 29th and another at the 50th aa) were made.

Additionally, a designed seven amino acids long sequence including a 6xHis-tag was added compared to variants addressed in this thesis (addition of the start codon or first seven original amino acids of LAAD). The enzyme folding was most likely facilitated by the formed secondary structures from the His-tag. If this was indeed the reason could be investigated in a next study.

4.5.4 Activity assays

Since no soluble expression of LAAD could be achieved, it was decided to use LAAD in a whole-cell approach for activity assays. The general question of LAAD enzyme classification was tested with two activity assays.

First a potential oxidase activity involving H₂O₂ production was examined [48]. As was already described in literature [43], no tested LAAD variant showed oxidase activity through building H₂O₂.

In the other assay a general oxidoreductase activity was applied. Therefore, suitable redox dyes indicating oxidoreduction by visible color change were investigated first [49]. In the course of testing DCPIP was found to be a highly useful redox indicator for LAAD reaction test. Methylene blue and methylene green were not suitable.

The protein concentrations of cell fractions (soluble, insoluble and membrane fraction) and their specific enzyme activity were determined. The highest average specific enzyme activities were measured in the membrane fraction followed by the insoluble fraction of LAAD expressing cells. These results confirmed the expectations of the enzyme localization experiments.

4.6 Conclusion and outlook

Three truncated enzyme variants were made and different factors of expression were tested. The designed truncated LAAD sequences were not leading to soluble expression of the enzyme. Two activity assays were then performed in a whole-cell environment. The known assumption of no H₂O₂ production could be reproduced and the redox dye DCPIP was found suitable for oxidoreductase activity testing.

It was later proven that soluble expression of LAAD is possible [57]. Thus, insights in the structure- function relationship and catalyzed reaction were delivered. These findings are expected to facilitate the way to the biocatalysis production of enantiomerically pure amino acids.

5 Abbreviations

A	absorption
aa	amino acids
AAP	4-aminoantipyrine
AldO	alditol oxidase
A-overhangs	adenine residue overhangs
bp	base pairs
BSA	bovine serum albumin
CaCl ₂	calcium chloride
CV	column volume
ddH ₂ O	double distilled water
DFF	2,5-furandicarboxaldehyde/ 2,5-diformylfuran
DNA	deoxyribonucleic acid
DNase I	deoxyribonuclease I
DCPIP	2,6-dichlorophenol-indophenol
DCHBS	3,5-dichloro-2-hydroxybenzenesulfonic acid
dLAAD	deleted/ truncated L-amino acid deaminase
dLAAD+A	dLAAD with adenine residue overhangs
ε	molar extinction coefficient
E50	elution imidazole buffer 50 mM
E500	elution imidazole buffer 500 mM
EC	enzyme class
<i>E. coli</i>	<i>Escherichia coli</i>
F	HMFO variant F352Y
FAD	flavin adenine dinucleotide
FADH ₂	reduced form of flavin adenine dinucleotide
FDCA	2,5-furandicarboxylic acid
FFA	5-formyl-2-furancarboxylic acid
FMN	flavin mononucleotide
HCl	hydrogen chloride
H ₂ O ₂	hydrogen peroxide
H	HMFO variant H333M
His	polyhistidine

HF	HMFO variant H333M/F352Y
HFVW	HMFO variant H333M/F352Y/ V367R/W466F
HMF	5-hydroxymethylfurfural
HmfH	HMF oxidoreductase from <i>Cupriavidus basilensis</i>
<i>hmfo</i>	gene of HMFO
HMFO	HMF oxidase
HRP	horseradish peroxidase
HPLC	high performance liquid chromatography
I	induced
IPTG	isopropyl- β -D-thiogalactoside
k_{cat}	turnover number
k_{cat}/K_M	catalytic efficiency
K_i	dissociation constant for substrate binding
K_M	Michaelis–Menten constant
KPi	potassium phosphate buffer
LAAD	L-amino acid deaminase
LB	lysogeny broth medium
L-phe	L-phenylalanine
MB	methylene blue
MG	methylene green
MgSO ₄	magnesium sulfate
NaCl	sodium chloride
Ni	nickel
O ₂	oxygen
OD ₆₀₀	optical density at 600 nm
o/n	overnight
ONC	overnight preculture
P	pellet
PCR	polymerase chain reaction
PEF	polyethylene furanoate
PET	polyethylene terephthalate
pH	potential of hydrogen
<i>P. myxofaciens</i>	<i>Proteus myxofaciens</i>
S	supernatant

SDS	sodium dodecyl sulfate
SDS-PAGE	sodium dodecyl sulfate polyacrylamide gel electrophoresis
SUMO	small ubiquitin-related modifier
TB	terrific broth medium
TMHMM	Tied Mixture Hidden Markov Model
Tris	tris(hydroxymethyl)aminomethane
rpm	revolutions per minute
U	unit in $\mu\text{M}/\text{min}$
UI	uninduced
UV	ultraviolet spectrum
UV/Vis	ultraviolet–visible spectrum
V	HMFO variant V367R
Vis	visible spectrum
V_{max}	maximum enzyme velocity
VW	HMFO variant V367R/W466F
W	HMFO variant W466F
W5	washing imidazole buffer 5 mM
W10	washing imidazole buffer 10 mM
WC	whole cell
w/v	weight per volume
WT	wildtype
v/v	volume per volume
YASARA	Yet Another Scientific Artificial Reality Application

6 References

- [1] V. Massey, "Activation of Molecular Oxygen by Flavins and Flavoproteins," *J. Biol. Chem.*, vol. 269, no. September 9, pp. 22459–22462, 1994.
- [2] B. G. Malmström, "Enzymology of oxygen," *Ann. Rev. Biochem.*, vol. 51, pp. 21–59, 1982.
- [3] P. K. Robinson, "Enzymes: principles and biotechnological applications," *Essays Biochem.*, vol. 59, no. 0, pp. 1–41, 2015.
- [4] P. MacHeroux, B. Kappes, and S. E. Ealick, "Flavogenomics - A genomic and structural view of flavin-dependent proteins," *FEBS J.*, vol. 278, no. 15, pp. 2625–2634, 2011.
- [5] P. Chaiyen and N. S. Scrutton, "Special Issue: Flavins and Flavoproteins: Introduction," *FEBS J.*, vol. 282, no. 16, pp. 3001–3002, 2015.
- [6] S. GHISLA and V. MASSEY, "Mechanisms of flavoprotein-catalyzed reactions," *Eur. J. Biochem.*, vol. 181, no. 1, pp. 1–17, 1989.
- [7] C. T. W. Moonen, J. Vervoort, and F. Müller, "Reinvestigation of the Structure of Oxidized and Reduced Flavin: Carbon-13 and Nitrogen-15 Nuclear Magnetic Resonance Study," *Biochemistry*, vol. 23, no. 21, pp. 4859–4867, 1984.
- [8] E. Romero, J. R. Gómez Castellanos, G. Gadda, M. W. Fraaije, and A. Mattevi, "Same Substrate, Many Reactions: Oxygen Activation in Flavoenzymes," *Chem. Rev.*, vol. 118, no. 4, pp. 1742–1769, 2018.
- [9] A. Mattevi, "To be or not to be an oxidase: challenging the oxygen reactivity of flavoenzymes," *Trends Biochem. Sci.*, vol. 31, no. 5, pp. 276–283, 2006.
- [10] V. Massey, M. Stankovich, and P. Hemmerich, "Light-Mediated Reduction of Flavoproteins with Flavins as Catalysts," *Biochemistry*, vol. 17, no. 1, pp. 1–8, 1978.
- [11] K. Yagi, "Chemical Determination of Flavins," *Methods Biochem. Anal.*, vol. 10, pp. 319–356, 1962.
- [12] A. Manuscript, "Plastics and Environmental Health : The Road Ahead," vol. 28, no. 1, pp. 1–8, 2014.
- [13] P. Frenzel, S. Fayyaz, R. Hillerbrand, and A. Pfennig, "Biomass as Feedstock in the Chemical Industry - An Examination from an Exergetic Point of View," *Chem. Eng. Technol.*, vol. 36, no. 2, pp. 233–240, 2013.
- [14] B. Erickson, Nelson, and P. Winters, "Perspective on opportunities in industrial

- biotechnology in renewable chemicals,” *Biotechnol. J.*, vol. 7, no. 2, pp. 176–185, 2012.
- [15] M. E. Davis, “Heterogeneous Catalysis for the Conversion of Sugars into Polymers,” *Top. Catal.*, vol. 58, no. 7–9, pp. 405–409, 2015.
- [16] Y.-T. Huang, J.-J. Wong, C.-J. Huang, C.-L. Li, and G.-W. B. Jang, “2,5-Furandicarboxylic Acid Synthesis and Use,” pp. 191–216, 2016.
- [17] C. Moreau, M. N. Belgacem, and A. Gandini, “Recent catalytic advances in the chemistry of substituted furans from carbohydrates and in the ensuing polymers,” *Top. Catal.*, vol. 27, no. 1–4, pp. 11–30, 2004.
- [18] K. M. Koeller and C. H. Wong, “Enzymes for chemical synthesis,” *Nature*, vol. 409, no. 6817, pp. 232–240, 2001.
- [19] F. Koopman, N. Wierckx, J. H. de Winde, and H. J. Ruijsenaars, “Efficient whole-cell biotransformation of 5-(hydroxymethyl)furfural into FDCA, 2,5-furandicarboxylic acid,” *Bioresour. Technol.*, vol. 101, no. 16, pp. 6291–6296, 2010.
- [20] W. P. Dijkman and M. W. Fraaije, “Discovery and characterization of a 5-hydroxymethylfurfural oxidase from *Methylovorus* sp. strain MP688,” *Appl. Environ. Microbiol.*, vol. 80, no. 3, pp. 1082–1090, 2014.
- [21] W. P. Dijkman, D. E. Groothuis, and M. W. Fraaije, “Enzyme-catalyzed oxidation of 5-hydroxymethylfurfural to furan-2,5-dicarboxylic acid,” *Angew. Chemie - Int. Ed.*, vol. 53, no. 25, pp. 6515–6518, 2014.
- [22] W. P. Dijkman, C. Binda, M. W. Fraaije, and A. Mattevi, “Structure-based enzyme tailoring of 5-hydroxymethylfurfural oxidase,” *ACS Catal.*, vol. 5, no. 3, pp. 1833–1839, 2015.
- [23] J. Carro, P. Ferreira, L. Rodríguez, A. Prieto, A. Serrano, B. Balcells, A. Ardá, J. Jiménez-Barbero, A. Gutiérrez, R. Ullrich, M. Hofrichter, and A. T. Martínez, “5-Hydroxymethylfurfural Conversion By Fungal Aryl-Alcohol Oxidase and Unspecific Peroxygenase,” *FEBS J.*, vol. 282, no. 16, pp. 3218–3229, 2015.
- [24] M. Theisen and J. C. Liao, “Industrial Biotechnology: *Escherichia coli* as a Host,” *Ind. Biotechnol. Microorg.*, pp. 149–181, 2017.
- [25] D. R. Cavener, “GMC oxidoreductases. A newly defined family of homologous proteins with diverse catalytic activities,” *J. Mol. Biol.*, vol. 223, no. 3, pp. 811–814, 1992.
- [26] A. L. Koch, “Turbidity measurements of bacterial cultures in some available

- commercial instruments,” *Anal. Biochem.*, vol. 38, no. 1, pp. 252–259, 1970.
- [27] M. Mandel and A. Higa, “Calcium-dependent bacteriophage DNA infection,” *J. Mol. Biol.*, vol. 53, no. 1, pp. 159–162, 1970.
- [28] Invitrogen and Invitrogen, “Champion pET SUMO Protein Expression System,” *Cloning*, vol. 5, no. January, pp. 75–86, 2004.
- [29] M. Singh, A. Yadav, X. Ma, and E. Amoah, “Plasmid DNA Transformation in Escherichia Coli: Effect of Heat Shock Temperature, Duration, and Cold Incubation of CaCl₂ Treated Cells,” *Shock*, vol. 6, no. 4, pp. 561–568, 2010.
- [30] H. Land and M. S. Humble, “Protein Engineering,” vol. 1685, pp. 43–67, 2018.
- [31] A. R. Shenoy and S. S. Visweswariah, “Site-directed mutagenesis using a single mutagenic oligonucleotide and DpnI digestion of template DNA,” *Anal. Biochem.*, vol. 319, no. 2, pp. 335–336, 2003.
- [32] W. P. Dijkman, “The kinetic mechanism of 5-(hydroxymethyl)furfural oxidase,” 2015.
- [33] J. X. Feliu, R. Cubarsi, and A. Villaverde, “Optimized release of recombinant proteins by ultrasonication of E. coli cells,” *Biotechnol. Bioeng.*, vol. 58, no. 5, pp. 536–540, 1998.
- [34] P. Macheroux, “UV-Visible Spectroscopy as a Tool to Study Flavoproteins,” in *Flavoprotein Protocols*, S. K. Chapman and G. A. Reid, Eds. Totowa, NJ: Humana Press, 1999, pp. 1–7.
- [35] A. Aliverti, B. Curti, and M. A. Vanoni, “Identifying and Quantitating FAD and FMN in Simple and in Iron-Sulfur-Containing Flavoproteins,” in *Flavoprotein Protocols*, S. K. Chapman and G. A. Reid, Eds. Totowa, NJ: Humana Press, 1999, pp. 9–23.
- [36] F. Forneris, R. Orru, D. Bonivento, L. R. Chiarelli, and A. Mattevi, “ThermoFAD, a Thermofluor-adapted flavin ad hoc detection system for protein folding and ligand binding,” *FEBS J.*, vol. 276, no. 10, pp. 2833–2840, 2009.
- [37] M. W. Pantoliano, E. C. Petrella, J. D. Kwasnoski, V. S. Lobanov, J. Myslik, E. Graf, T. Carver, E. Asel, B. A. Springer, P. Lane, and F. R. Salemme, “High-Density Miniaturized Thermal Shift Assays as a General Strategy for Drug Discovery,” *J. Biomol. Screen.*, vol. 6, no. 6, pp. 429–440, 2001.
- [38] H. van de Waterbeemd, M. Kansy, B. Wagner, and H. Fischer, “Lipophilicity Measurement by Reversed-Phase High Performance Liquid Chromatography (RP-HPLC),” pp. 73–87, 2008.

- [39] O. S. Wolfbeis, "Luminescent sensing and imaging of oxygen: Fierce competition to the Clark electrode," *BioEssays*, vol. 37, no. 8, pp. 921–928, 2015.
- [40] F. Forneris, R. Orru, D. Bonivento, L. R. Chiarelli, A. Mattevi, W. P. Dijkman, C. Binda, M. W. Fraaije, A. Mattevi, D. R. Tobergte, S. Curtis, W. P. Dijkman, C. Binda, M. W. Fraaije, A. Mattevi, H. Land, M. S. Humble, Invitrogen, and Invitrogen, "Champion pET SUMO Protein Expression System," *J. Chem. Inf. Model.*, vol. 5, no. January, pp. 1833–1839, 2015.
- [41] S. Ghisla, A. Wenz, and C. Thorpe, "Suicide Substrates as Irreversible Inhibitors of Aavoenzymes," *Enzyme*, no. March, pp. 43–60, 1980.
- [42] I. Ilisz, R. Berkecz, and A. Péter, "Application of chiral derivatizing agents in the high-performance liquid chromatographic separation of amino acid enantiomers: A review," *J. Pharm. Biomed. Anal.*, vol. 47, no. 1, pp. 1–15, 2008.
- [43] D. P. Pantaleone, A. M. Geller, and P. P. Taylor, "Purification and characterization of an L -amino acid deaminase used to prepare unnatural amino acids," *J. Mol. Catal. B*, vol. 11, pp. 795–803, 2001.
- [44] W. P. Dijkman, G. De Gonzalo, A. Mattevi, and M. W. Fraaije, "Flavoprotein oxidases: Classification and applications," *Appl. Microbiol. Biotechnol.*, vol. 97, no. 12, pp. 5177–5188, 2013.
- [45] D. Matsui, D. H. Im, A. Sugawara, Y. Fukuta, S. Fushinobu, K. Isobe, and Y. Asano, "Mutational and crystallographic analysis of l-amino acid oxidase/monooxygenase from *Pseudomonas* sp. AIU 813: Interconversion between oxidase and monooxygenase activities," *FEBS Open Bio*, vol. 4, pp. 220–228, 2014.
- [46] C. W. V. Gmbh, C. Kгаа, and R. S. Enantiopure, "Biocontrolled Formal Inversion or Retention of l - a -Amino Acids to," 2014.
- [47] A. Krogh, B. Larsson, G. Von Heijne, and E. L. L. Sonnhammer, "Predicting transmembrane protein topology with a hidden Markov model: Application to complete genomes," *J. Mol. Biol.*, vol. 305, no. 3, pp. 567–580, 2001.
- [48] D. P. H. M. Heuts, E. W. Van Hellemond, D. B. Janssen, and M. W. Fraaije, "Discovery, characterization, and kinetic analysis of an alditol oxidase from *Streptomyces coelicolor*," *J. Biol. Chem.*, vol. 282, no. 28, pp. 20283–20291, 2007.
- [49] D. Brugger, I. Krondorfer, K. Zahma, T. Stoisser, J. M. Bolivar, B. Nidetzky, C.

- K. Peterbauer, and D. Haltrich, "Convenient microtiter plate-based, oxygen-independent activity assays for flavin-dependent oxidoreductases based on different redox dyes," *Biotechnol. J.*, vol. 9, no. 4, pp. 474–482, 2014.
- [50] K. C. Lin, C. Y. Yin, and S. M. Chen, "An electrochemical biosensor for determination of hydrogen peroxide using nanocomposite of poly(methylene blue) and FAD hybrid film," *Sensors Actuators, B Chem.*, vol. 157, no. 1, pp. 202–210, 2011.
- [51] S. García-Castiñeiras, S. Velázquez, P. Martínez, and N. Torres, "Aqueous humor hydrogen peroxide analysis with dichlorophenol-indophenol," *Experimental Eye Research*, vol. 55, no. 1, pp. 9–19, 1992.
- [52] M. M. Bradford, "A rapid and sensitive method for the quantitation of microgram quantities of protein utilizing the principle of protein-dye binding," *Anal. Biochem.*, vol. 72, no. 1–2, pp. 248–254, 1976.
- [53] G. L. Rosano and E. A. Ceccarelli, "Recombinant protein expression in Escherichia coli: Advances and challenges," *Front. Microbiol.*, vol. 5, no. APR, pp. 1–17, 2014.
- [54] M. Zoonens and B. Miroux, "Expression of Membrane Proteins at the Escherichia coli Membrane for Structural Studies," in *Heterologous Expression of Membrane Proteins: Methods and Protocols*, I. Mus-Veteau, Ed. Totowa, NJ: Humana Press, 2010, pp. 49–66.
- [55] G. Gourinchas, E. Busto, M. Killinger, N. Richter, B. Wiltschi, and W. Kroutil, "A synthetic biology approach for the transformation of L- α -amino acids to the corresponding enantiopure (R)- or (S)- α -hydroxy acids," *Chem. Commun.*, vol. 51, no. 14, pp. 2828–2831, 2015.
- [56] L. Dumon-Seignovert, G. Cariot, and L. Vuillard, "The toxicity of recombinant proteins in Escherichia coli: A comparison of overexpression in BL21(DE3), C41(DE3), and C43(DE3)," *Protein Expr. Purif.*, vol. 37, no. 1, pp. 203–206, 2004.
- [57] P. Motta, G. Molla, L. Pollegioni, and M. Nardini, "Structure-function relationships in L-amino acid deaminase, a flavoprotein belonging to a novel class of biotechnologically relevant enzymes," *J. Biol. Chem.*, vol. 291, no. 20, pp. 10457–10475, 2016.